Three-Dimensional Neutronics for a Fusion Power Plant Non-Mobile Gas-Cooled Solid Blanket

M.M.H. Ragheb and C.W. Maynard

February 7, 1975

UWFDM-92

FUSION TECHNOLOGY INSTITUTE

UNIVERSITY OF WISCONSIN

MADISON WISCONSIN

Three-Dimensional Neutronics for a Fusion Power Plant Non-Mobile Gas-Cooled Solid Blanket

M.M.H. Ragheb and C.W. Maynard

Fusion Technology Institute
University of Wisconsin
1500 Engineering Drive
Madison, WI 53706

http://fti.neep.wisc.edu

February 7, 1975

UWFDM-92

Three-Dimensional Neutronics Cell Calculations for a Fusion Reactor Gas-Cooled Solid Blanket

Magdi M. H. Ragheb and Charles W. Maynard

January, 1977

Department of Nuclear Engineering
The University of Wisconsin
Madison, Wisconsin 53706

UWFDM-92 (Revised)

Acknowledgement: Research partially supported by the Energy Resource and Development Agency and the Wisconsin Electric Utility Research Foundation. The discrete ordinates calculation for the benchmark problem in the appendix was kindly carried out by Y. Gohar and T. Wu. M. Abdou helpfully provided the cross sections data for the Monte Carlo computations.

Foreword

This is a revision of the original report - the revision is required by the study of further cases. Modifications to the earlier estimates for the standard deviations are added. Here, independence between the contributions to the tritium breeding by different reactions and in different regions is assumed. Attention is called to the larger amounts of structural material imposed by mechanical and heat transfer considerations; than were accounted for, in the one-dimensional discrete-ordinates calculations. The heterogeneity effect and the neutron leakage to the shield are also emphasized. The objective of the three dimensional calculation is to account for these factors, and as such, the calculational model, and results, differ substantially from those of the one-dimensional calculations. A benchmark calculation compares results obtained by discrete ordinates to those obtained by the revised version of the used Monte Carlo code for the one-dimensional standard blanket model, and establishes the validity of the three-dimensional results obtained.

TABLE OF CONTENTS

ABSTRACT

Neutronics cell calculations for a solid gas-cooled fusion power plant blanket are investigated by three-dimensional Monte Carlo. The analysis suggests that such a design behaves strongly as a heterogeneous system. Satisfactory values of tritium breeding per (D-T) reaction can be achieved by proper design. In a parametric study, some cases yield values of the gross blanket breeding ratio around 1.06. This value differs substantially from that predicted by one-dimensional calculations. Toroidal effects are not accounted for since they are not expected to significantly influence integral effects such as the breeding ratio or total energy production; but the energy leakage in specific directions will be affected.

Improved designs should involve minimizing neutron leakage to the magnet shields and parasitic neutron absorption by the structure, by appropriate compositions and configurations. Optimization by three-dimensional computations is necessary for achieving satisfactory tritium breeding in solid blankets. Higher values of the breeding ratio should be attained to accomodate for uncertainties in the data, and for plant and reprocessing losses.

A one-dimensional comparative benchmark calculation establishes the validity of the three-dimensional results.

1. INTRODUCTION

In the present work, three-dimensional models for Monte-Carlo computations are used for neutronics studies of the gas-cooled solid blanket concept adopted for the UWMAK-II, Tokamak conceptual power plant design. The result is an iterated design compared to the earlier results based on the previous one-dimensional discrete-ordinates computations.[1,3]

Tritium breeding-energy absorbing blankets are a basic design feature of fusion power plants. A principal constituent of the blanket is the element, lithium, with isotopes Li-6 and Li-7, which can be transmuted to tritium through the reactions Li-6(n,T)He-4 and Li-7(n,n' + T)He-4.

Solid gas-cooled blankets for fusion power plants offer the advantages of low lithium and tritium inventories, and an easy tritium recovery achieved by high tritium concentrations. Helium appears to be a suitable choice as a coolant, avoiding temperature, pressure or compatibility limitations of other coolants.[1,2,3] Type 316-Stainless Steel is a good choice as a structural material for a near-term, present-day technology power plant.[1,3] The choice of $LiAlO_2$ as a breeding material offers the advantages of a high melting point, and an acceptable tritium diffusion coefficient[1,3,4].

A cross section view of the power reactor design considered is shown in Figure 1. Lithium in the breeding material is enriched to 90 per cent in Li-6, and slow neutrons dominate the tritium breeding process. There exists a necessity for a neutron multiplier material. Metallic beryllium was the best choice for this function. Graphite was chosen as a suitable reflector material.

The first wall is protected against erosion by charged particle bombardment by both a poloidal divertor and a two-dimensional woven-carbon curtain cloth mounted on the vacuum chamber wall. This also protects the plasma from high-Z impurities.

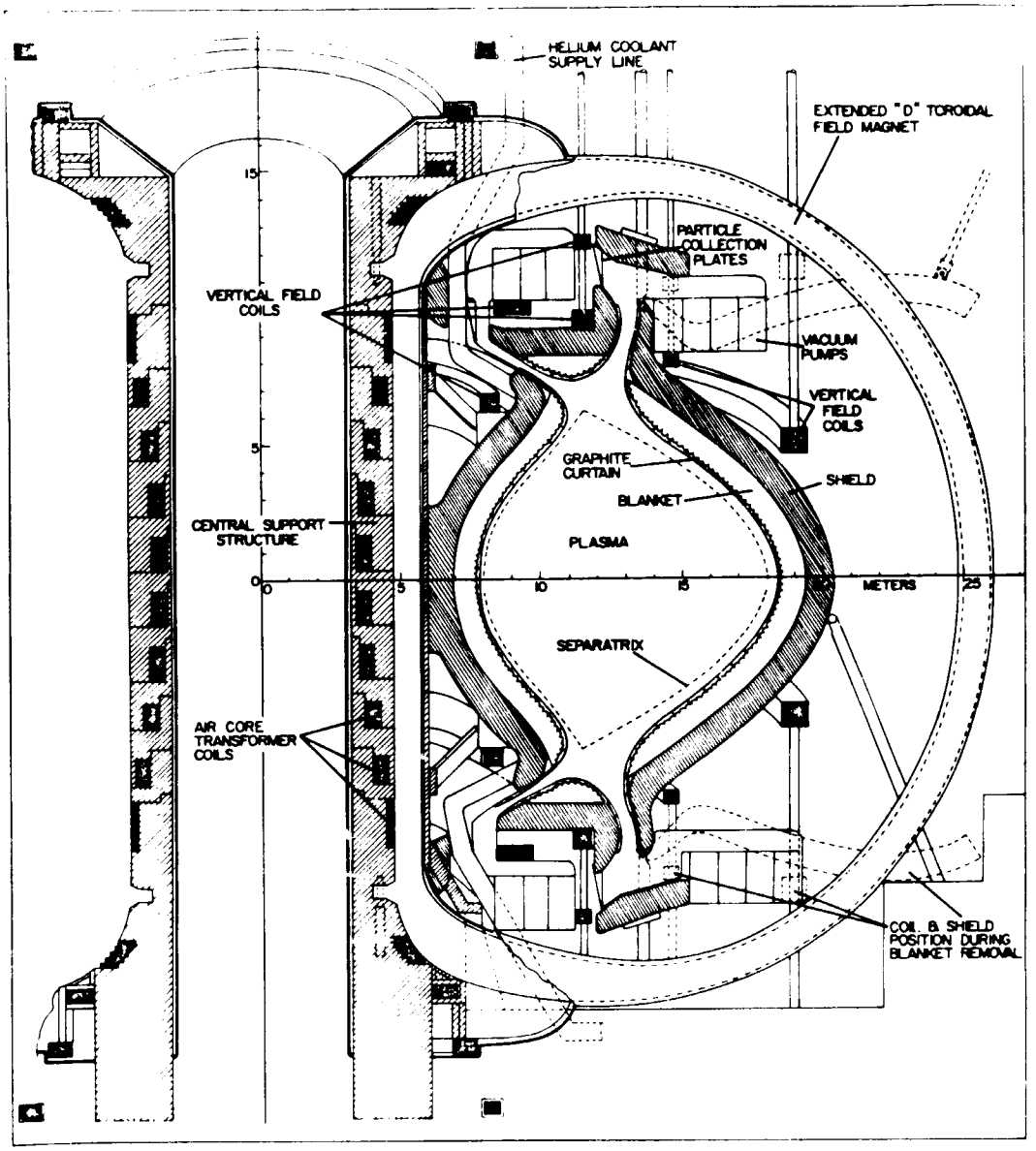

Figure 1. Vertical cross section view of UWMAK-II

The problem considered is the determination of the amount of tritium produced in the blanket since a design is not acceptable unless the tritium production exceeds the consumption rate. The amount of excess production (to allow for process losses, sale, etc) is an important factor in comparing competing concepts.

In section 2, the gas-cooled solid blanket configuration is described. Materials compositions are described in section 3.2 and cross section data in section 3.3. In sections 3.4 and 3.5, two computational models, a microcell and a macrocell, are given for the blanket, along with the computed results. The macrocell model is recommended for treatment of most problems. Some parametric studies suggesting alternative designs are also described in section 3.5. Section 4 compares Monte-Carlo results to discrete ordinates one-dimensional results for a similar system[1,3], obtained using the ANISN[8] code, as well as a Monte-Carlo computation and another discrete-ordinates computation for a liquid lithium cooled system.[9]

Conclusions and recommendations for future developments are given in section 5. It appears from these results that gas-cooled solid blanket systems behave as a heterogeneous system, and that three-dimensional calculations are necessary for dependable neutronics results. One-dimensional discrete-ordinate computations tend to overestimate the blanket breeding ratio by neglecting the heterognenity effect. This contrasts to liquid metal cooled systems, where one-dimensional discrete-ordinate models may be adequate[9], even though neglecting effects of penetrations (divertor slots and beam injection ports).

In this work, we preferred the notation: "blanket breeding ratio" to mean what is commonly referred to in the literature as the "breeding ratio", since the latter implies a knowledge of tritium consumption and losses which are not treated here. It is suggested to distinguish between:

i) The "gross blanket breeding ratio," treated in this work.

ii) The "net blanket breeding ratio," accounting for neutrons missing the blanket and passing through the divertor slots, and pellet and beam injection ports.

iii) The "plant breeding ratio,", related to an overall plant mass balance.

The adopted macrocell three-dimensional model for the blanket reference design analyzed here predicts an adequate breeding artio (gross) of: 1.067 ± 0.026 compared to a value of 1.184 predicted by the one-dimensional discrete ordinates model, for the original blanket system. The present design differs from the one-dimensional design by the presence of a larger amount of structural material imposed by mechanical and heat transfer design considerations.

Parametric studies show that larger blanket breeding ratios can be obtained with the addition of extra neutron multiplier (Be). Further iterations on the materials, heat transfer and structural design could lead to near optimal, high performance solid gas-cooled blanket designs as proposed in section 5. Optimization of the compositions and volumes of the zone is necessary.

2. BLANKET CONFIGURATION

Horizontal and vertical cross sections through one of the blanket cells are shown in Figures 2 and 3.

The blanket is constructed of cells in which the lithium aluminate and beryllium are enclosed in stainless steel cylinders having a 3.75 cm outer diameter and a 0.09 cm wall thickness. Preceding the graphite zone, these tubes are closed at one end and attached to a small gas plenum at the other end for tritium collection. The graphite reflector is canned in stainless steel and cooled by the main helium coolant stream.(1)

The maximum pressure of the helium coolant in the blanket is 50 atm, the total energy per fusion is 18 Mev per D-T neutron. The use of a solid breeding

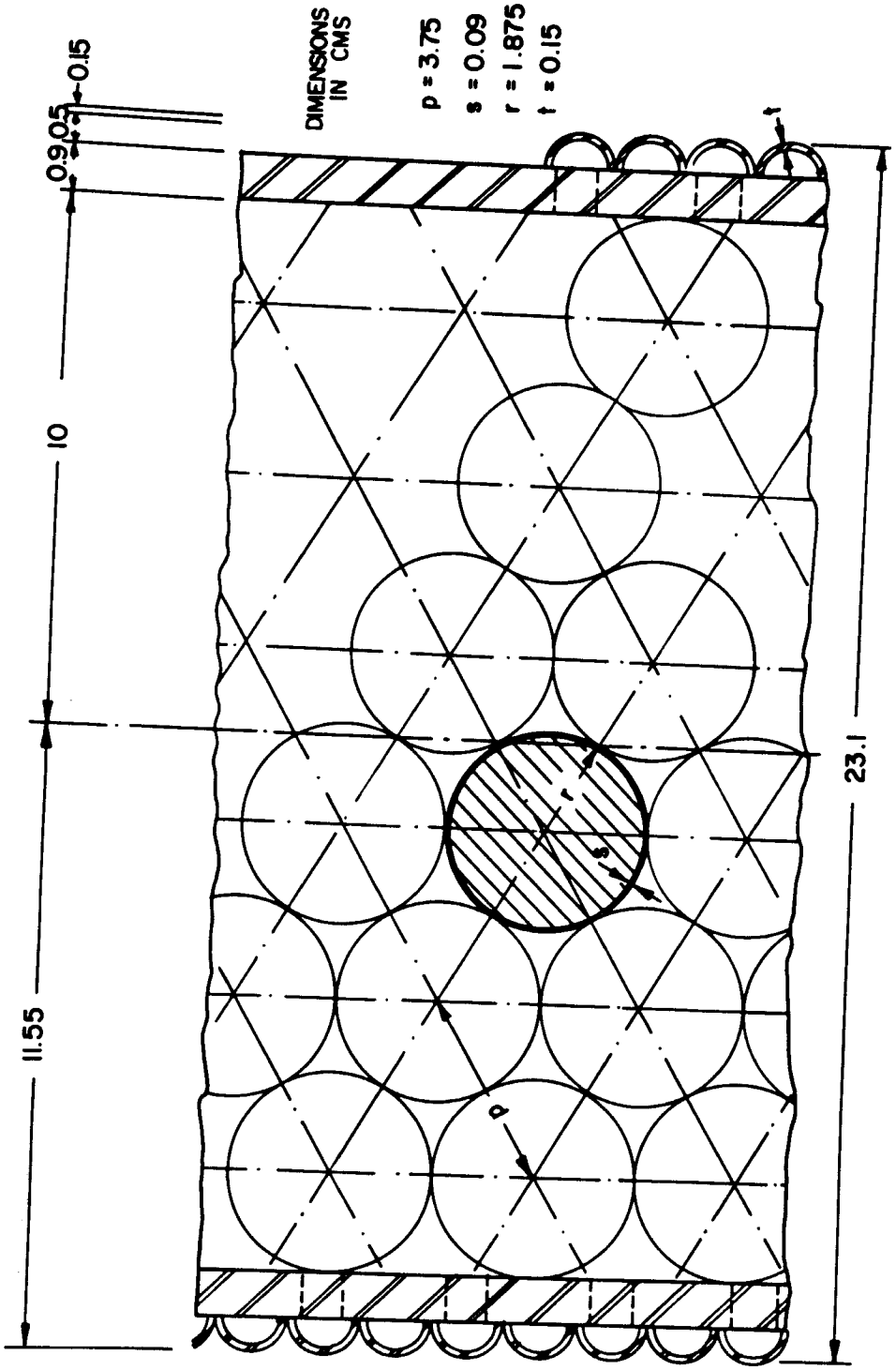

Figure 2

Horizontal cross-section through solid breeder cell

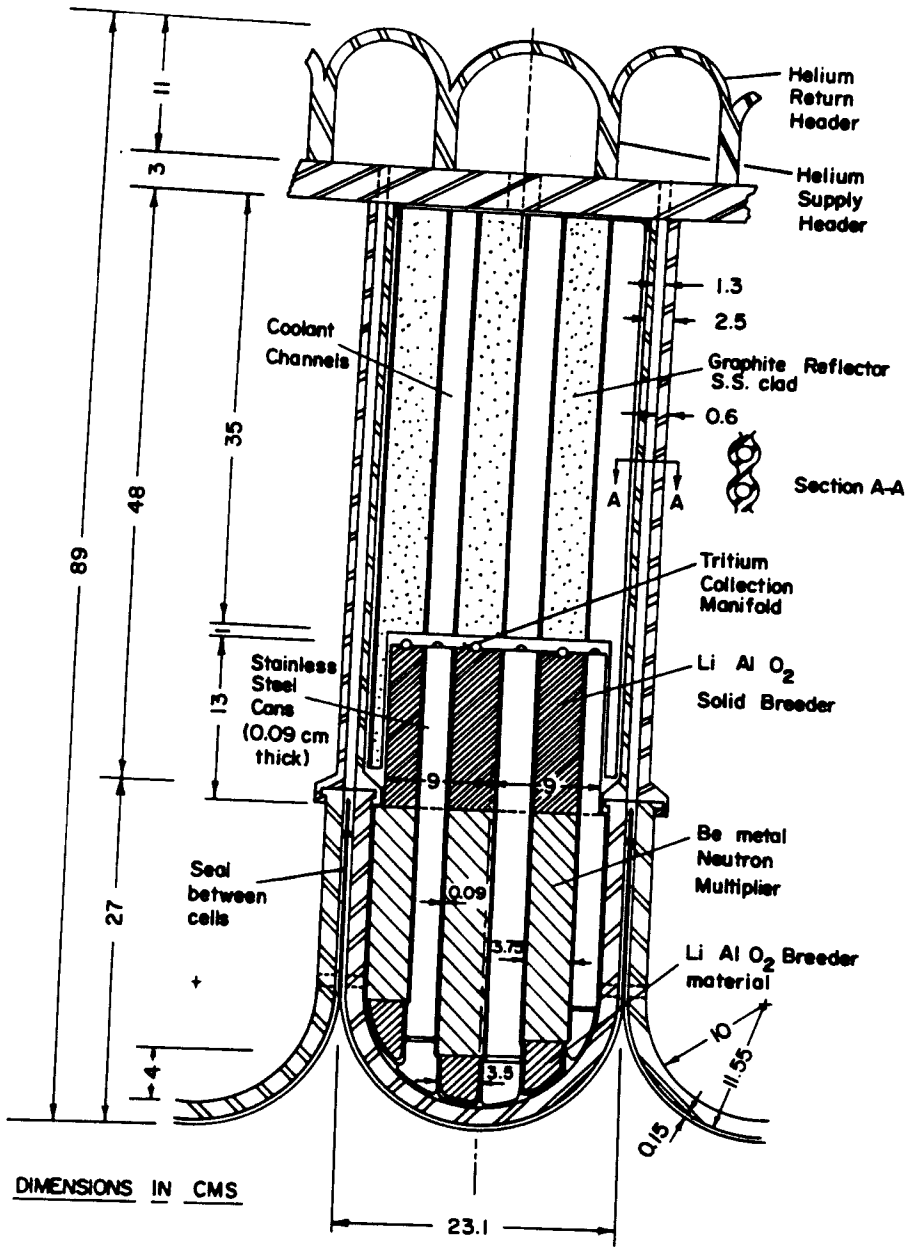

Figure 3 Vertical Section through solid blanket cells

material: $LiAlO_2$, 90% enriched in Li^6, results in a large tritium production cross section which reduces the low energy neutron mean free path significantly, and leads to a low lithium inventory in the blanket (~4.1×10^4kg compared with 1.4×10^6kg in the earlier UWMAK-I design). Due to easier tritium removal, this results in a low tritium inventory. The tritium inventory in the blanket[3] is about 40 gm, compared to 8.7 kg in the liquid lithium breeder-coolant concept. Breeding with Li^6 is achieved by slow neutrons, and a neutron multiplier (Be) is needed for neutron multiplication. The neutron multiplying zone is placed between two breeding zones of lithium aluminate.

The surface temperature of the stainless steel clad pins containing $LiAlO_2$ is found to be about 600°C. The centerline temperature is over 1300°C. The resulting diffusion coefficient limits the tritium path to about 10 microns which requires the lithium aluminate to be either a powder of ~20 μm diameter particles or a porous medium with pores about 20 μm apart.

Mechanically the blanket consists of three major parts: the removable front wall cells, the vertical structure connecting the front wall cells to the He headers, and the He gas headers themselves. The removable front wall consists of a 0.9 cm thick backing capable of carrying the pressure stresses in the cylindrical cell and a thinner, 0.15 cm thick section enclosing small semi-circular tubes 1 cm in inner diameter running perpendicular to the cell and electron-welded to the 0.9 cm backing. This scheme allows a maximum design stress of 8500 psi for the first wall.[1] The vertical structure, 48 cm high, anchors front wall cells to the headers, and contains conduits for He gas going to the front wall. This structure is welded to the bottom header plate and, together with the headers, constitutes a stiff support sustaining the vacuum load on the blanket wall.[1]

3. THREE-DIMENSIONAL MONTE-CARLO NEUTRONICS CELL CALCULATIONS

3.1 Introduction

The helium cooled solid blanket for the UWMAK-II conceptual design is analyzed neutronically. Two three-dimensional models were tried. A microcell model treated in section 3.4 was found to underestimate the neutron absorption by the lateral stainless steel structure even though it took into account heterogeneity effects which could not be analyzed by one-dimensional discrete ordinates calculations. A macrocell model discussed in section 3.5 is thought to best represent such solid gas-cooled blanket concepts. Materials compositions adopted in the models and cross section data used in the computations are discussed in sections 3.2 and 3.3 respectively.

3.2 Materials Compositions

Type 316 stainless steel was considered to consist of the following materials with their corresponding atomic densities:

316 Stainless Steel (100% density factor):	Chromium	0.014 500 atoms/(barn·cm)
	Nickel	0.009 380 atoms/(barn·cm)
	Iron	0.061 410 atoms/(barn·cm)

These atomic densities are further modified by appropriate density factors (to be introduced later) for the different stainless steel zones.

The lithium aluminate (with 90% enriched lithium-6) atomic densities were taken as:

$LiAlO_2$ (90% enriched Li^6): (90% density factor)	3-Li-6	0.018 873 atoms/(barn·cm)
	3-Li-7	0.002 097 atoms/(barn·cm)
	Oxygen	0.041 940 atoms/(barn·cm)
	Aluminum	0.020 970 atoms/(barn·cm)

The beryllium and graphite atomic densities adopted are:

Graphite (90% density factor)	Carbon 0.0723	atoms/(barn·cm)
Beryllium (90% density factor)	Beryllium 0.1112	atoms/(barn·cm)

The He coolant having a very low density: 1.663×10^{-4} gm/cm^3 (20°C, 1 atm), and a very small cross section was considered as a vacuum.

These number densities were adopted from a previous one-dimensional discrete ordinates calculation.[1]

3.3 Cross Section Data

The multigroup neutron cross sections were in the form of the 46-group structure shown in Table I. These were collapsed from the GAM-II one hundred group structure using typical CTR blanket spectra. The 46 group data structure has the same five group structure above 2 MeV as the one hundred group set.[2] These data were originally obtained as the DLC-2[10] data package from RSIC. The DLC-Library was generated by the program SUPERTOG from nuclear data in ENDF/B version III.[11,13]

A P_3 scattering anisotropy was used throughout the computations. The DLC-29 /MACKLIB[12], RSIC data library was used to obtain reaction cross sections for the tritium breeding reactions, which were subsequently collapsed to the 46-group structure. The identifications of the tritium breeding reactions used are:

i) $3Li^6$, MAT 1115, MT 107, N°82 Reaction 7(n,α), Q = +.4786(+7)ev

ii) $3Li^7$, MAT 1116, MT 91,LR33, N°83, Reaction 5(n,n') to continuum (n,n')T, Q = -.2466(+7)ev

iii) Be^9, MAT 1154, MT 105, N°87, Reaction 6(n,t), Q = -.1043(+8)ev

Table I

Neutron 46 Energy Group Structure

Group	Group Limits E(Top)	E(Low)	E(Mid Point)	Upper Lethargy
1	1.4918 (+7)*	1.3499 (+7)	1.4208 (+7)	-0.4
2	1.3499 (+7)	1.2214 (+7)	1.2856 (+7)	-0.3
3	1.2214 (+7)	1.1052 (+7)	1.1633 (+7)	-0.2
4	1.1052 (+7)	1.0000 (+7)	1.0526 (+7)	-0.1
5	1.0000 (+7)	9.0484 (+6)	9.5242 (+6)	0.0
6	9.0484 (+6)	8.1873 (+6)	8.6178 (+6)	0.1
7	8.1873 (+6)	7.4082 (+6)	7.7979 (+6)	0.2
8	7.4082 (+6)	6.7032 (+6)	7.0557 (+6)	0.3
9	6.7032 (+6)	6.0653 (+6)	6.3843 (+6)	0.4
10	6.0653 (+6)	5.4881 (+6)	5.7787 (+6)	0.5
11	5.4881 (+6)	4.9659 (+6)	5.2270 (+6)	0.6
12	4.9659 (+6)	4.4933 (+6)	4.7296 (+6)	0.7
13	4.4933 (+6)	4.0657 (+6)	4.2795 (+6)	0.8
14	4.0657 (+6)	3.6788 (+6)	3.8722 (+6)	0.9
15	3.6788 (+6)	3.3287 (+6)	3.5038 (+6)	1.0
16	3.3287 (+6)	3.0119 (+6)	3.1703 (+6)	1.1
17	3.0119 (+6)	2.7253 (+6)	2.8686 (+6)	1.2
18	2.7253 (+6)	2.4660 (+6)	2.5956 (+6)	1.3
19	2.4660 (+6)	1.8268 (+6)	2.1251 (+6)	1.4
20	1.8268 (+6)	1.3534 (+6)	1.5743 (+6)	1.7
21	1.3534 (+6)	1.0026 (+6)	1.1663 (+6)	2.0
22	1.0026 (+6)	7.4274 (+5)	8.6401 (+6)	2.3
23	7.4274 (+5)	5.5023 (+5)	6.4008 (+5)	2.6
24	5.5023 (+5)	4.0762 (+5)	4.7418 (+5)	2.9
25	4.0762 (+5)	3.0197 (+5)	3.5128 (+5)	3.2
26	3.0197 (+5)	2.2371 (+5)	2.6024 (+5)	3.5
27	2.2371 (+5)	1.6573 (+5)	1.9279 (+5)	3.8
28	1.6573 (+5)	1.2277 (+5)	1.4282 (+5)	4.1
29	1.2277 (+5)	6.7379 (+4)	9.8803 (+4)	4.4
30	6.7379 (+4)	3.1828 (+4)	4.6671 (+4)	5.0

Table I (continued)

Group	Group Limits E(Top)	E(Low)	E(Mid Point)	Upper Lethargy
31	3.1828 (+4)	1.5034 (+4)	2.2046 (+4)	5.75
32	1.5034 (+4)	7.1017 (+3)	1.0414 (+4)	6.50
33	7.1017 (+3)	3.3546 (+3)	4.9191 (+3)	7.25
34	3.3546 (+3)	1.5846 (+3)	2.3236 (+3)	8.00
35	1.5846 (+3)	7.4852 (+2)	1.0976 (+3)	8.75
36	7.4852 (+2)	3.5358 (+2)	5.1847 (+2)	9.50
37	3.5358 (+2)	1.6702 (+2)	2.4491 (+2)	10.25
38	1.6702 (+2)	7.8893 (+1)	1.1569 (+2)	11.00
39	7.8893 (+1)	3.7267 (+1)	5.4647 (+1)	11.75
40	3.7267 (+1)	1.7603 (+1)	2.5813 (+1)	12.50
41	1.7603 (+1)	8.3153 (+0)	1.2193 (+1)	13.25
42	8.3153 (+0)	3.9279 (+0)	5.7597 (+0)	14.00
43	3.9279 (+0)	1.8554 (+0)	2.7207 (+0)	14.75
44	1.8554 (+0)	8.7643 (-1)	1.2852 (+0)	15.50
45	8.7643 (-1)	4.1399 (-1)	6.0707 (-1)	16.25
46	4.1399 (-1)	2.200 (-2)	2.1800 (-1)	17.00
			Lowest	20.00

* $(\pm n)$ represents $(10^{\pm n})$

E in ev

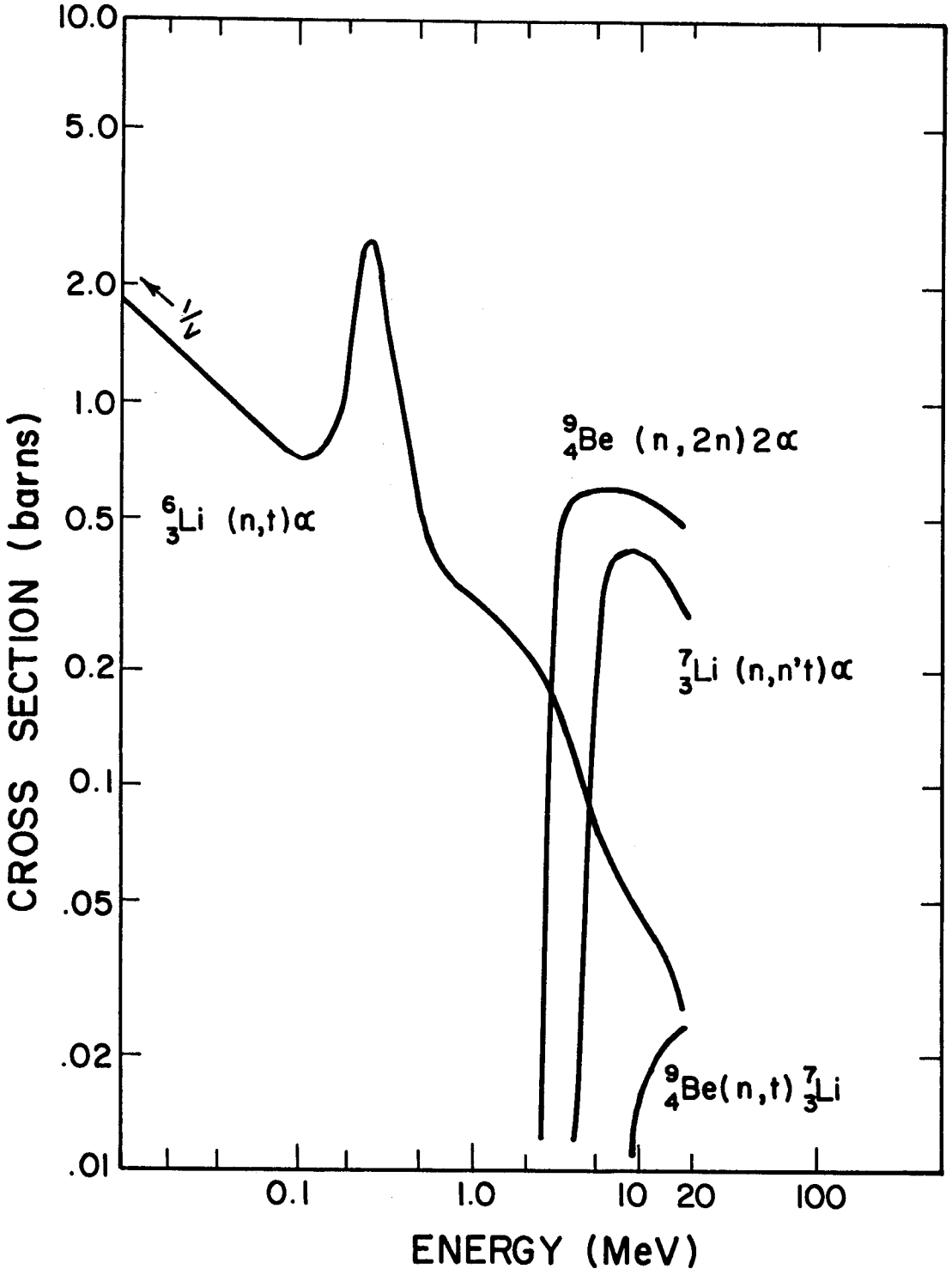

Figure 4 Comparison of cross sections for major tritium production reactions, and neutron multiplication reaction

Table II

Reaction Cross Sections in Barns for Tritium Production
(46-group structure)

Group	$3Li^6(n,t)\alpha$	$3Li^7(n,n't)\alpha$	$4Be^9(n,t)Li^7$
1	2.5604-02	3.2948-01	1.9939-02
2	2.8380-02	3.5947-01	9.4005-03
3	3.2337-02	3.8789-01	2.1440-04
4	3.5937-02	4.0816-01	0.0000
5	4.0158-02	4.1637-01	
6	4.5338-02	4.2090-01	
7	5.0600-02	4.2386-01	
8	5.6601-02	4.1878-01	
9	6.3480-02	3.9913-01	
10	7.0939-02	3.5898-01	
11	7.9822-02	2.5548-01	
12	8.8645-02	1.2057-01	
13	9.9173-02	4.5174-01	
14	1.1159-01	1.6963-02	
15	1.2464-01	8.8833-03	
16	1.3701-01	3.0915-03	
17	1.5406-01	1.1390-03	
18	1.7757-01	0.0000	
19	2.0432-01		
20	2.3363-01		
21	2.5653-01		
22	2.7184-01		
23	2.9115-01		
24	3.8586-01		
25	8.7261-01		
26	2.7388+00		
27	1.9399+00		
28	8.8067-01		
28	6.6739-01		
30	7.4849-01		

Table II (continued)

Group	$3Li^{6}(n,t)\alpha$	$3Li^{7}(n,n't)\alpha$	$4Be^{9}(n,t)Li^{7}$
31	1.0312+00	0.0000	0.0000
32	1.4806+00		
33	2.1453+00		
34	3.1203+00		
35	4.5426+00		
36	6.6064+00		
37	9.6315+00		
38	1.4021+01		
39	2.0408+01		
40	2.9702+01		
41	4.3224+01		
42	6.2904+01		
43	9.1519+01		
44	1.3321+02		
45	1.9381+02		
46	5.4458+02		

Tritium is produced principally through the Li-6(n-T) He-4 reaction, which has a large $1/v$ thermal cross section (940.25 barns at 0.025 ev) and a resonance peak of 2.71 barns at 247 kev.

These reaction cross sections are tabulated in Table II, and displayed in Figure 4. Table III shows the ENDF/B MAT and the DLC-29 ID identification numbers for the materials used in our computations.

3.4 Microcell Model

In this three-dimensional model, a unit cell at the center of the breeding cells was chosen for analysis. Horizontal and vertical cross sections through such a cell are shown in Figures 5 and 6. This model will be discussed briefly since it was not found to adequately describe the system. Table IV shows the tritium production per (D-T) reaction by this model in different breeding materials and zones.

An estimate of the blanket breeding ratio (gross) for the reference design was obtained as: 1.148 ± 0.027 compared to a value of 1.184 resulting from a one-dimensional discrete ordinates computation (though the three dimensional model contains more $LiAlO_2$ and Be). Such a difference may be attributed to two reasons:

1) A neutron-streaming from the blanket to the shield caused by the tubular configuration. The neutron escape probability from the cell was estimated as 0.030.

2) A strong parasitic absorption of slow neutrons by the stainless steel cans is noted which lowers the tritium production, since these slow neutrons would otherwise be used for breeding with Li^6.

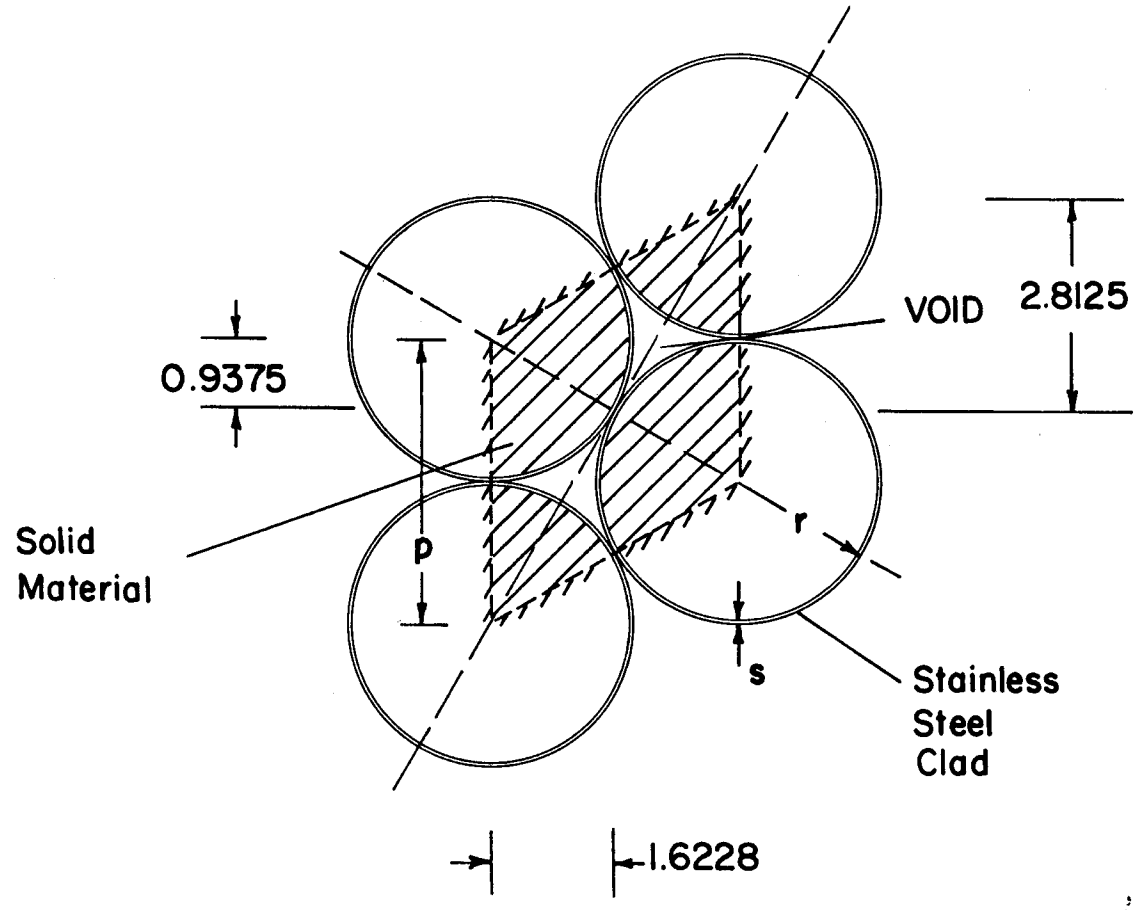

p = 3.75

s = 0.03

r = 1.875

DIMENSIONS IN CMS

SCALE 1:1

Figure 5: Horizontal cross section through microcell model

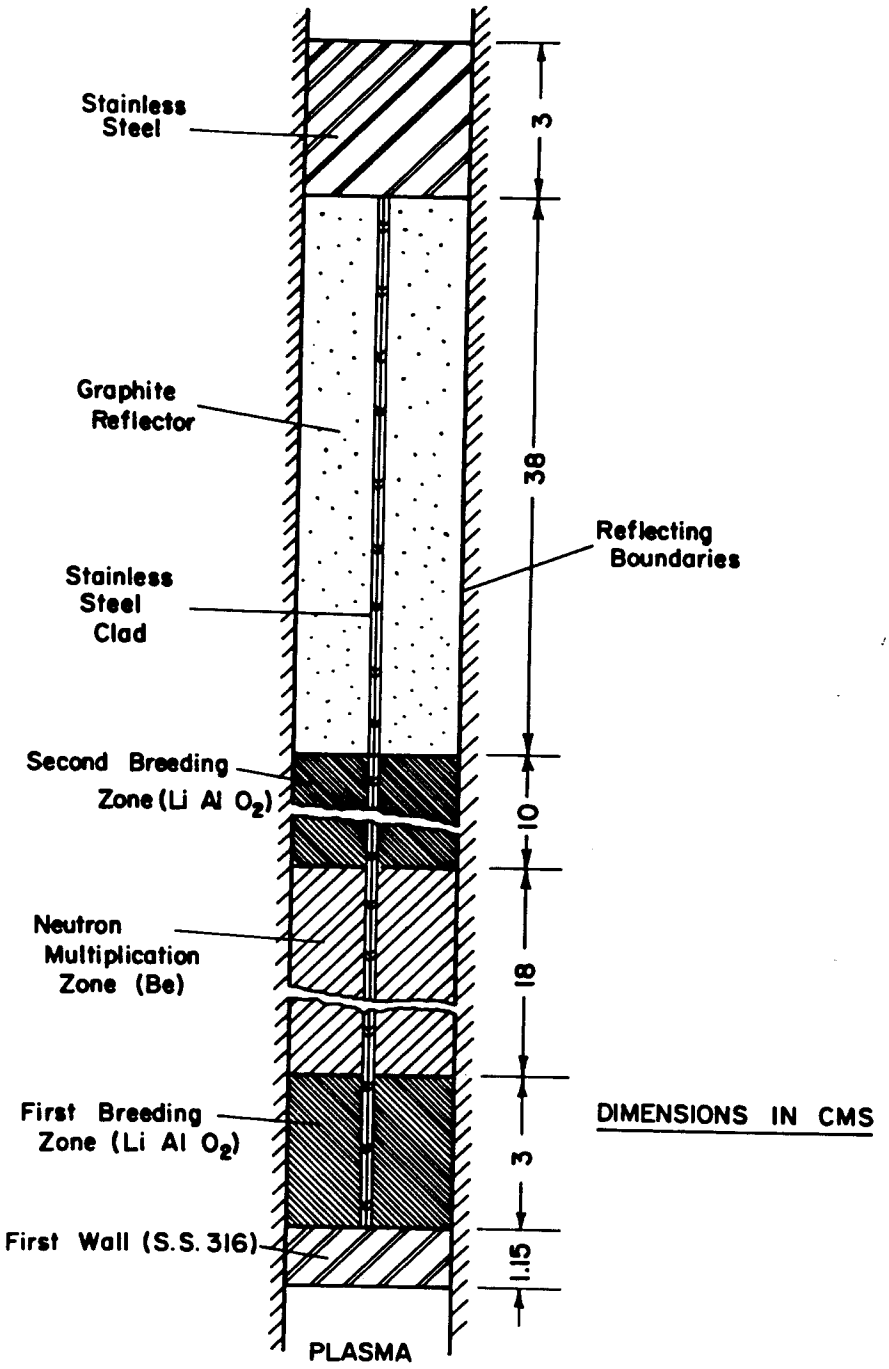

Figure 6: Vertical Cross Section of Microcell Model

TABLE III

Identifications for materials used in UWMAK-II blanket:

Associated ENDF/B MAT numbers, and ID numbers in DLC-29/MACKLIB Library

Material	ENDF/B MAT	DLC-29 ID
Li-6	1115	5115
Li-7	1116	5116
Be-9	1154	5154
C-12	1165	5165
O-16	1134	5134
Al-27	1135	5135
Cr	1121	5121
Fe	1180	5180
Ni	1123	5123

TABLE IV

Tritium production per (D-T) reaction estimate by the microcell model

$N(Li^6) = 0.018873 \left[\frac{\text{atoms}}{\text{barn. cm}}\right]$ (90% d.f.)

$N(Li^7) = 0.002097 \left[\frac{\text{atoms}}{\text{barn. cm}}\right]$ (90% d.f.)

$N(Be^9) = 0.074130 \left[\frac{\text{atoms}}{\text{barn. cm}}\right]$ (60% d.f.)

escape probability = 0.029804

$\Delta t_2(LiAlO_2) = 10$ cm

$\Delta t_1(LiAlO_2) = 3$ cm

Number of histories = 1500

Zone / Contribution from	First Lithium Aluminate Zone	Beryllium Zone	Second Lithium Aluminate Zone	Total Contribution
Li^6	0.553267±0.022992	-	0.582946±0.014112	1.136213±0.026977
Li^7	0.002939±0.000017	-	0.001295±0.000132	0.004234±0.000133
Be^9	-	0.007645±0.000355	-	0.007645±0.000355
Total Contribution	0.556206±0.022992	0.007645±0.000	0.584241±0.014112	1.148092±0.026980

This model disregards the effect of the stainless steel in the lateral structure (coolant inlet to the first wall tubing and support structure), and the curvature of the first wall, so that the macrocell model was set up to investigate their effect on the breeding process.

3.5 Macrocell Model

In this three-dimensional model, a unit cell was chosen as shown in Figures 7, 8 and 9. Lithium aluminate is contained in stainless steel cans 0.09 cm thick in two regions: VIII and XI. Beryllium also is contained in stainless steel tubes in regions IX and X. Region V represents the first wall tubing, and region VI represents the stainless steel gas coolant inlet tubing and support structure. The atomic densities of materials in these zones were adjusted to account for the actual amounts of materials in these regions. Regions VII and XIII represent the tritium collection manifold and coolant inlet and outlet ports respectively. Region XII is graphite contained in stainless steel tubing. Region compositions and atomic densities are displayed in Table VIII. Such a geometry represents adequately the actual blanket configuration shown in Figure 3.

The geometry module of the MORSE code was used to represent that geometry and an output of the PICTURE routine showing a section through the lithium aluminate and beryllium zones with the cladding and first wall stainless steel zones is shown in Figure 10.

Russian Roulette was used for particles reaching 1/1000 of their original weight, and results of calculations are announced in the form

$$\theta \pm S$$

where S is the estimated standard deviation

θ is the estimated mean value.

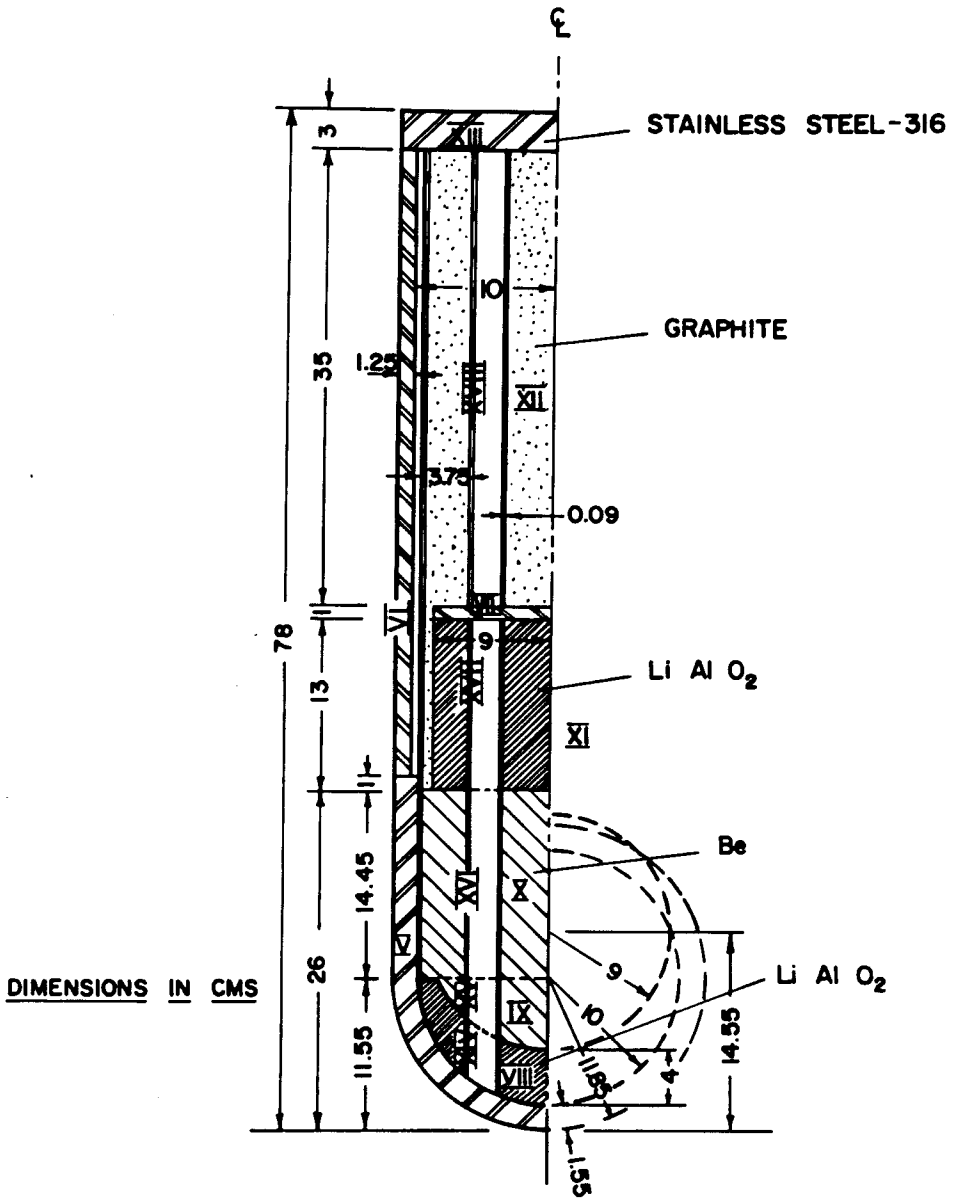

Figure 7 Vertical cross section through macrocell model

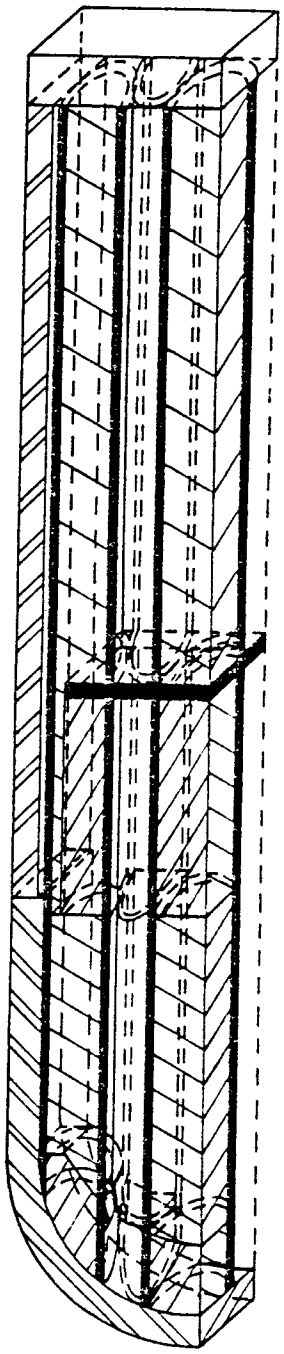

Figure 8 Blanket unit cell configuration, vertical cut

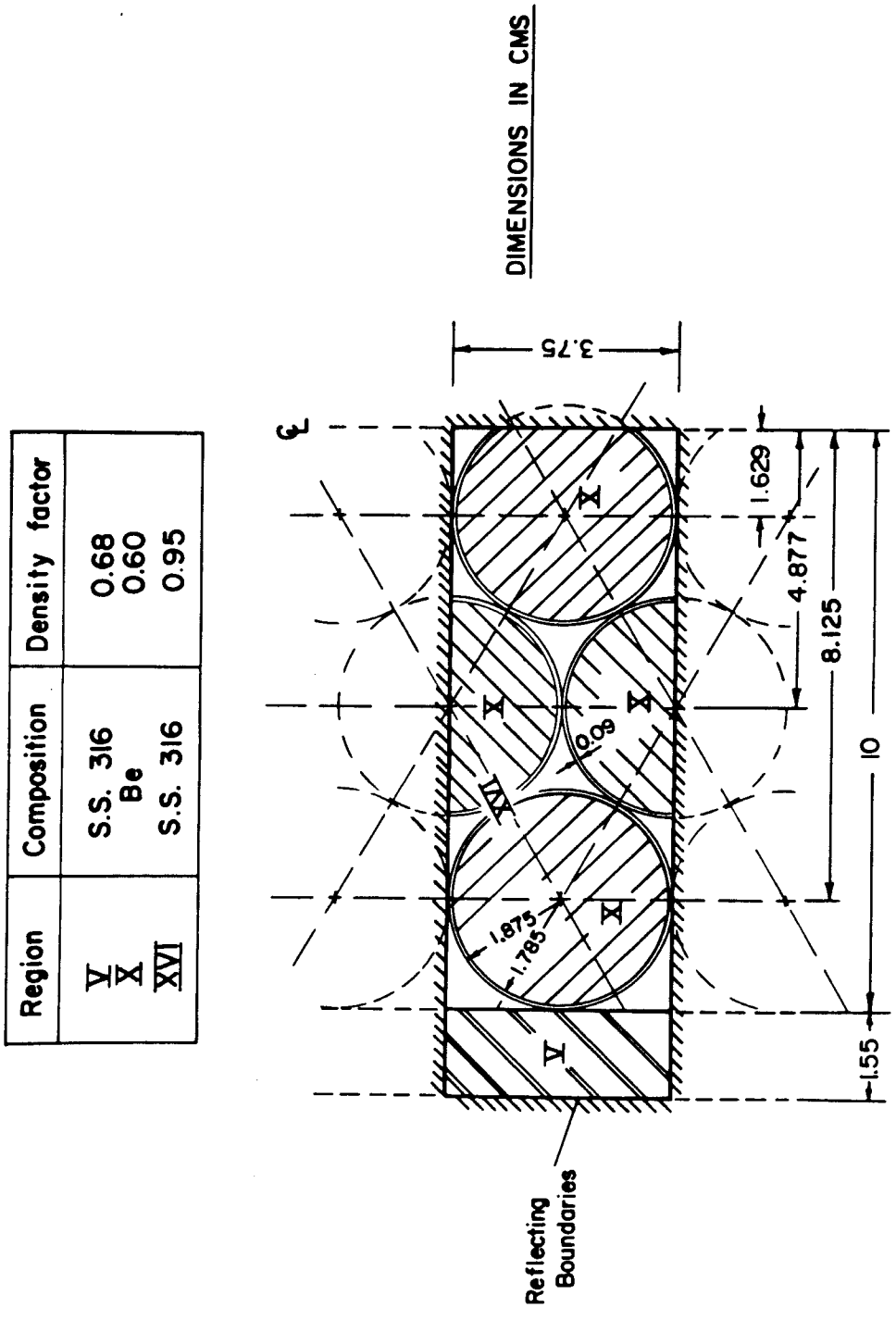

Figure 9 Horizontal section through macrocell model (Be zone)

* Stainless steel 316 Wall

2,3 Stainless steel 316 Clad

= $LiAlO_2$

\+ Be

0 Reflecting boundaries

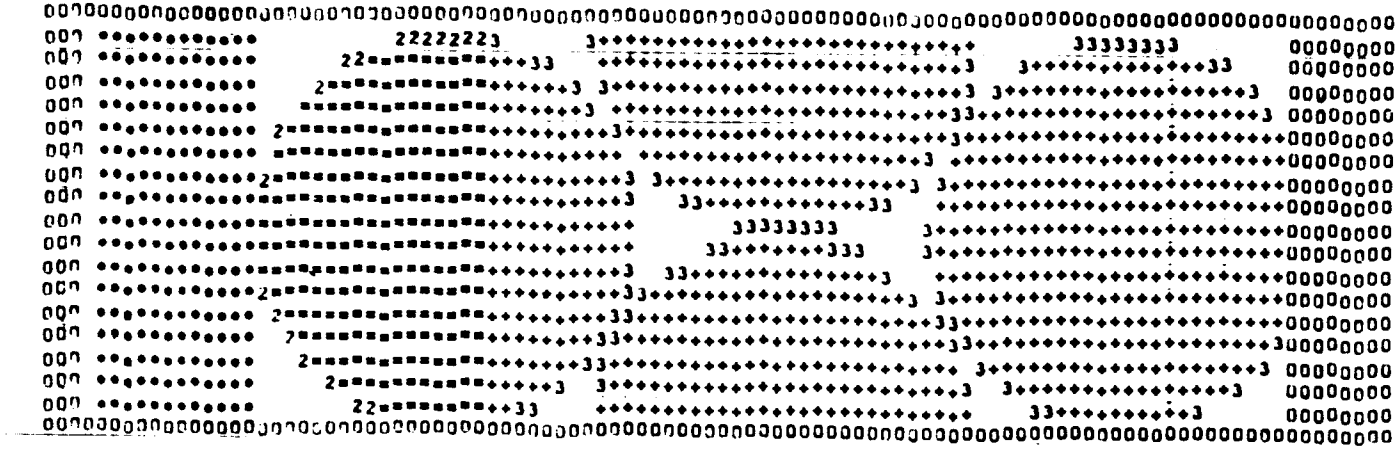

Figure 10 A Picture Routine Output Showing a Section through the $LiAlO_2$ and Be zones in a unit macrocell

This corresponds to a 68.2% confidence interval. If a 95.4% confidence interval is required, the form $\theta \pm 2S$ should be used.

The blanket breeding ratio (gross) in different zones is displayed in Table V. This blanket design was chosen on the basis of a parametric study to be discussed below, and yields a blanket breeding ratio (gross) of 1.067 ± 0.026. The escape probability for neutrons was 0.046. The blanket breeding ratio (gross) is satisfactory, but the neutron escape requires more shielding and cooling at the back of the breeding cells.

3.6 Parametric Studies

Important neutronics phenomena were uncovered in these studies. Numerical results show that solid gas cooled blankets behave basically as a heterogeneous system, and that three-dimensional calculations are important for adequate design of such systems. Near optimal designs can be achieved by suitable material configurations and compositions. The neutron economy is highly affected by the large amount of structural materials present.

The neutron escape probability from the blanket to the shield is sensitive to the quantity of Be neutron multiplier, the thickness of the graphite reflector and the quantity of lithium aluminate breeding material. The escape probability not only decreases with additional graphite, as would be expected, but also with the addition of Be which shows that beryllium also acts as a strong moderator and reflector, in addition to acting as a neutron multiplier. Neutrons slowed down in the Be may be scattered back to the first lithium aluminate zone, or forward to the second lithium aluminate zone where they interact with the Li^6 for tritium production.

Table V

Effect of Varying the Amount of Lithium Aluminate on the Blanket Breeding Ratio (Gross)

(Second Lithium Aluminate Zone - 13 cm, Graphite Reflector - 35 cm)

Designs A and B

$N(Be^9) = 0.074130$ 60% d.f.†

Design A: $LiAlO_2$ 60% d.f. : $N(Li^6) = 0.012582$ (atoms/(barn·cm)) escape probability = 0.045769
$N(Li^7) = 0.001398$ (atoms/(barn·cm)) (1000 histories)

Design B: $LiAlO_2$ 90% d.f. : $N(Li^6) = 0.018873$ (atoms/(barn·cm)) escape probability = 0.039686
$N(Li^7) = 0.002097$ (atoms/(barn·cm)) (2000 histories)

Material \ Zone		First $L_iA_1O_2$ Zone	Beryllium Zone	Second $L_iA_1O_2$ Zone	Total Contribution
Li^6	A	0.570105 ± 0.019783	---	0.481085 ± 0.017107	1.057190 ± 0.026153
	B	0.569021 ± 0.011602	---	0.481243 ± 0.009836	1.050264 ± 0.015210
Li^7	A	0.002507 ± 0.000149	---	0.000759 ± 0.000114	0.003266 ± 0.000187
	B	0.003244 ± 0.000085	---	0.000840 ± 0.000073	0.004084 ± 0.000112
Be^9	A	---	0.007028 ± 0.000406	---	0.007028 ± 0.000406
	B	---	0.005592 ± 0.000236	---	0.005592 ± 0.000236
Total	A	0.578612 ± 0.019783	0.007028 ± 0.000406	0.481844 ± 0.017107	1.067484 ± 0.026157
	B	0.572265 ± 0.011602	0.005592 ± 0.000236	0.482083 ± 0.009836	1.059940 ± 0.015212

† d.f. = density factor

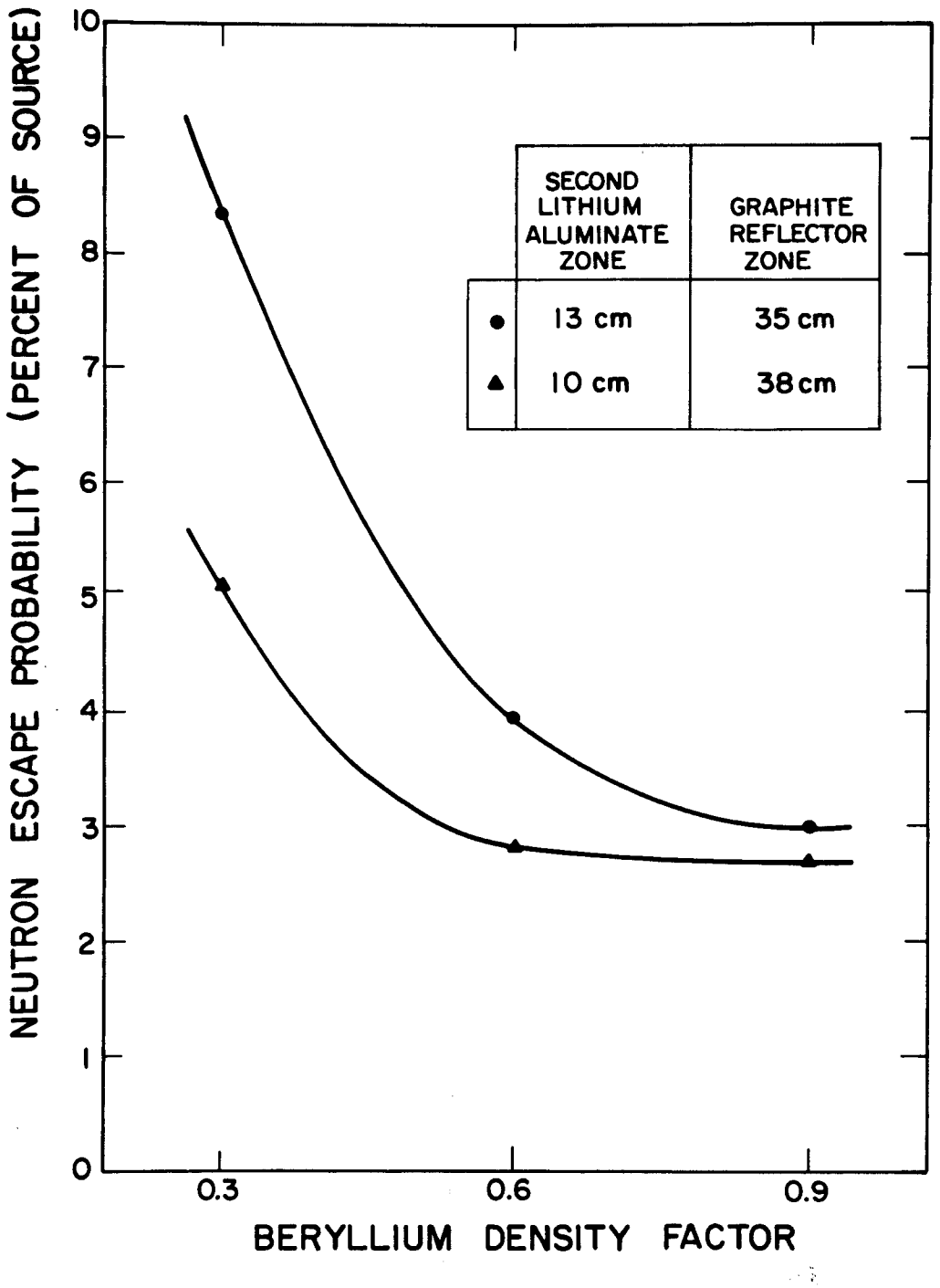

Figure 10: Neutron escape probability for different thicknesses of the breeding and reflecting zones. Design B results.

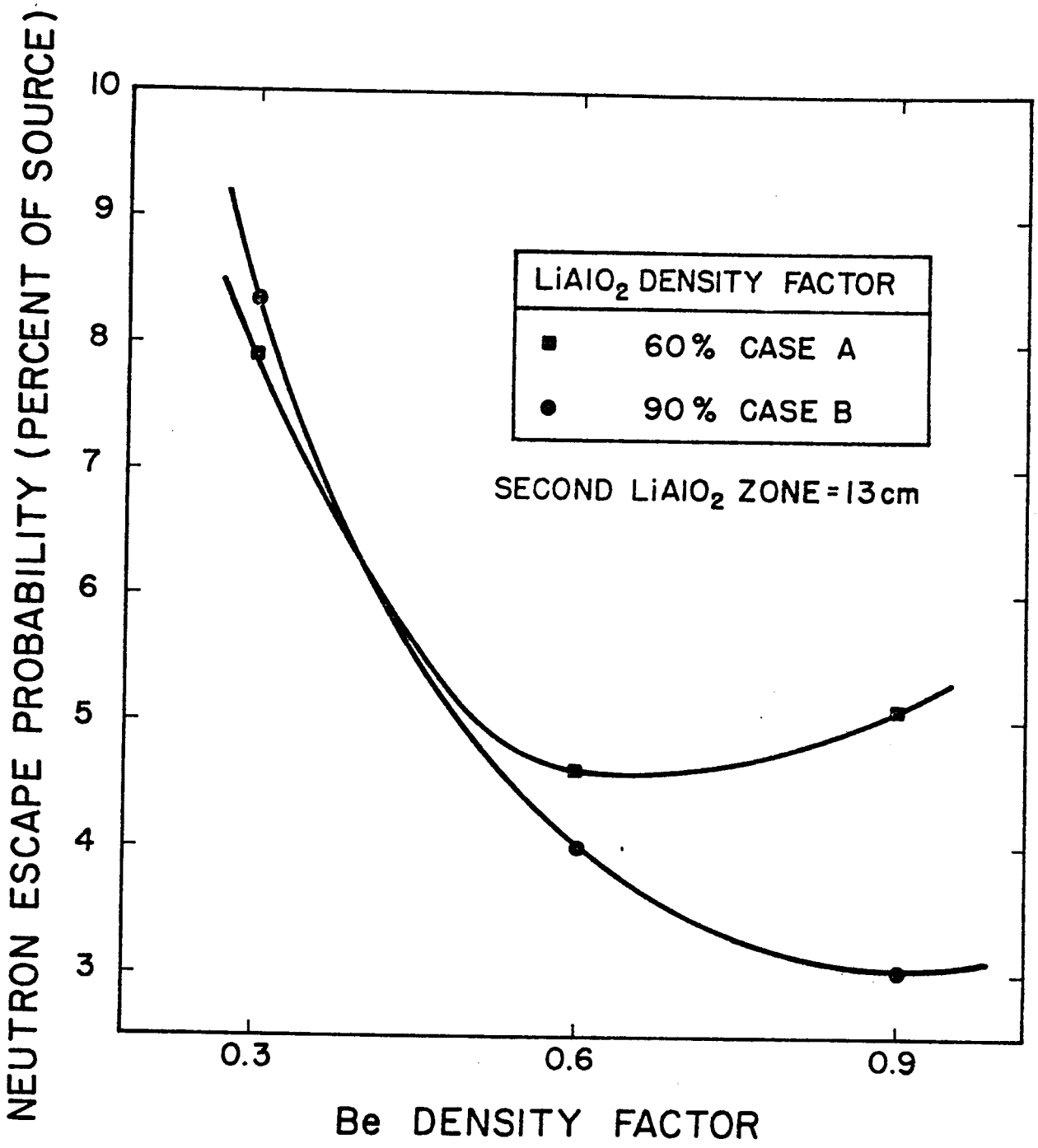

Figure 11. Neutron escape probability. Comparison of Designs A and B.

However, these moderated neutrons do not contribute to further neutron multiplication in the Be and have a probability of being parasitically absorbed in the stainless steel structure and lost with respect to the breeding process. The behavior of the neutron escape probability is shown in Figures 10 and 11. This is defined as :

$$\text{Neutron escape probability} = \frac{\text{Total weight of neutrons escaping blanket}}{\text{Total weight of neutrons impinging on 1st wall}}$$

The first lithium aluminate zone and the beryllium zone, see two neutron currents - an incoming one from the plasma, and a reflected one from subsequent material layers.

Each material layer has a reflection and a transmission coefficient for neutrons of different energies. Added to the reflector action of the graphite, the Be multiplier also reflects neutrons back to the first breeding zone. Tritium breeding in the second breeding zone is sensitive to the optical thickness of the first breeding zone. Figures 12 and 13 show that optimizing the optical thickness of the first breeding zone, enhances tritium breeding by the increase of neutron multiplication in the Be zone. Increasing the amount of breeding material in the second breeding zone also increases tritium production.

The above remarks were inferred from estimates of the tritium atom production per (D-T) reaction for different cases of lithium aluminate, graphite and beryllium thicknesses. Results of 3 cases are shown in Tables VI, VII and VIII. The scalar flux in different regions is displayed in Table IX for the blanket designs A and B. A comparison is shown in Table V. The first and second analyzed cases correspond to design B, the third to design A. Designs A and B mostly differ in the amount of Lithium Aluminate present, as accounted for by its density factor.

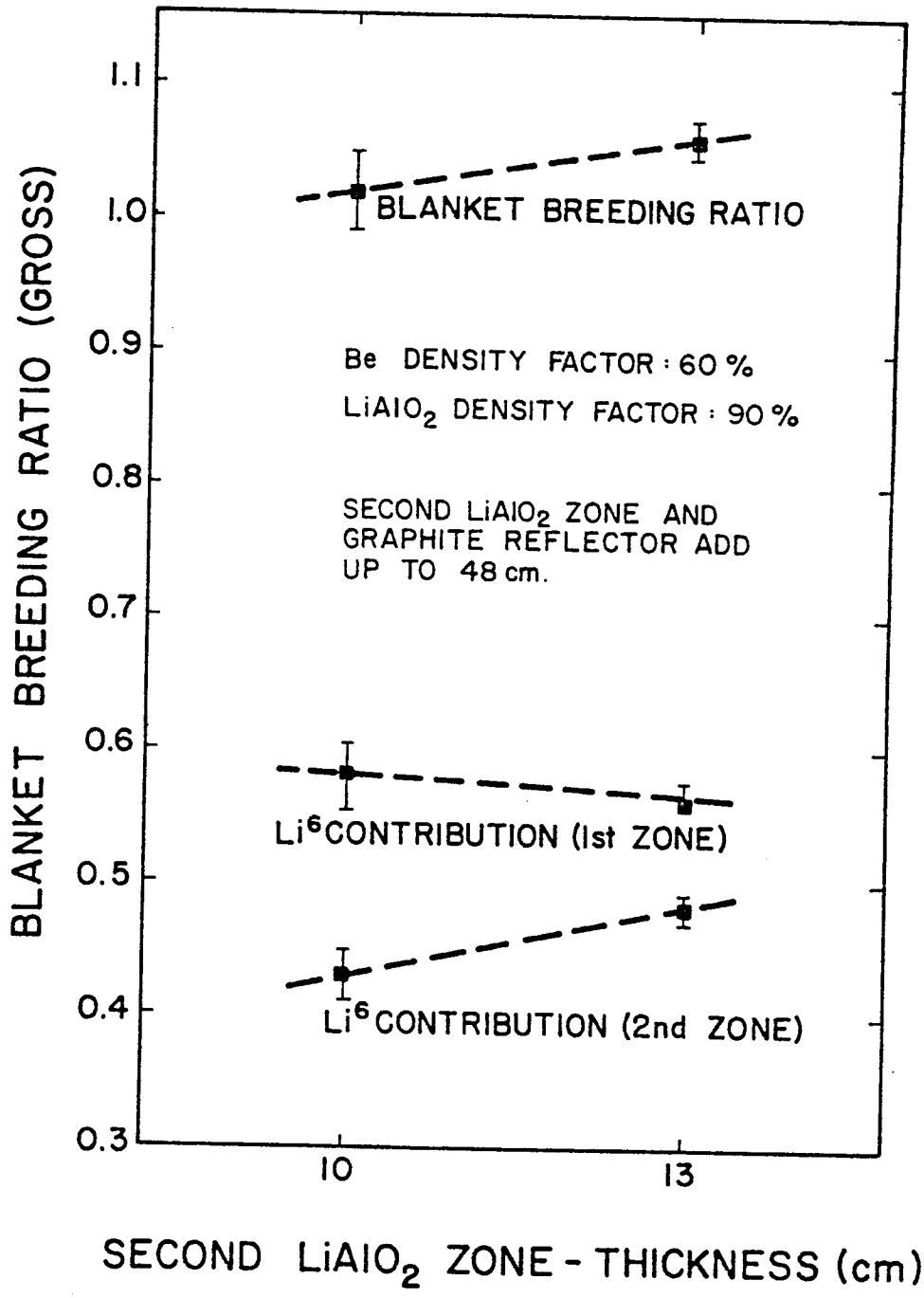

Figure 12: Effect of thickness of second L_iAlO_2 zone on tritium breeding.

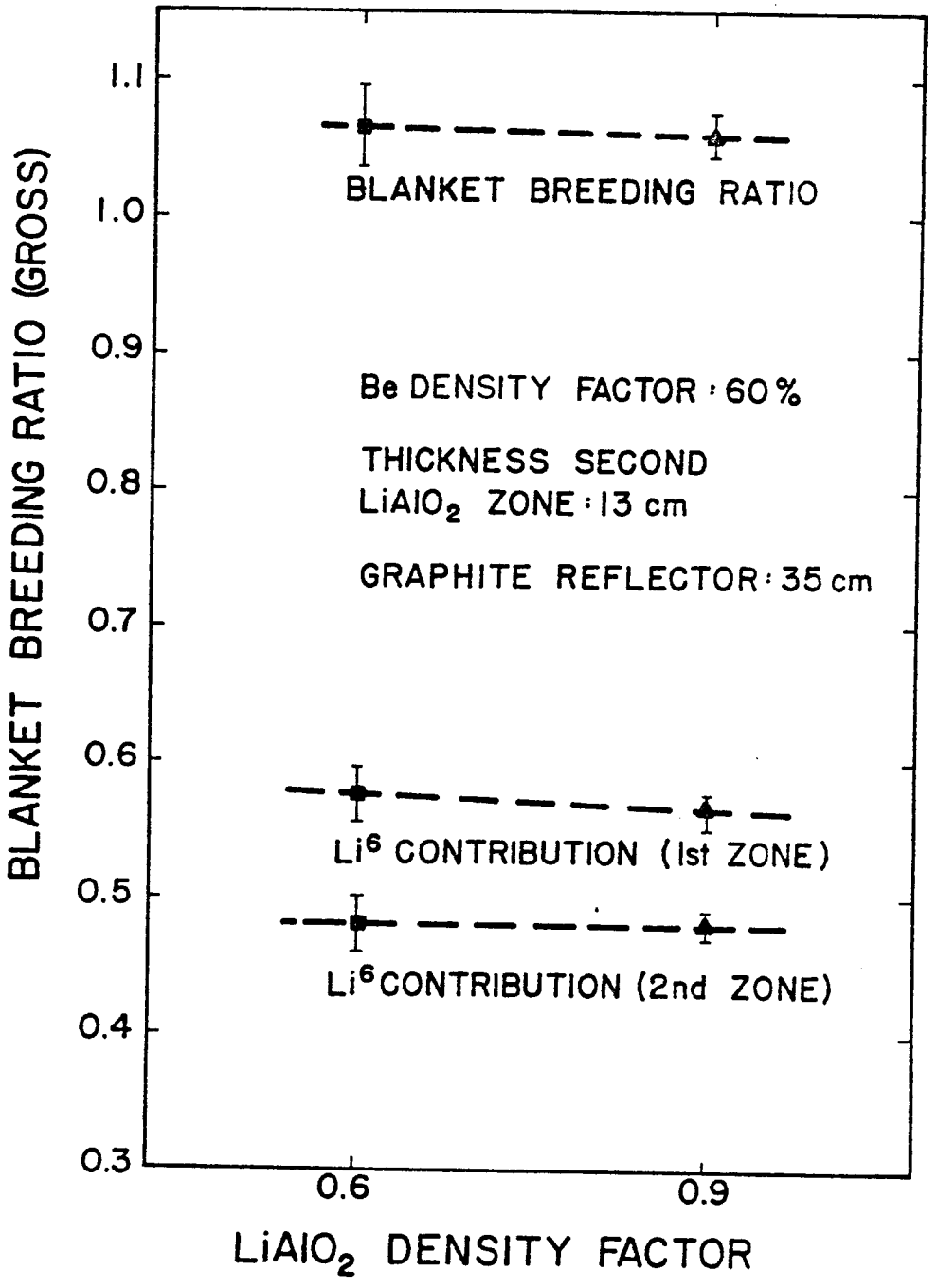

Figure 13: Effecto of L_iAlO_2 density factor on blanket breeding ratio.

Table VI

Effect of Changing the Amount of Beryllium on Blanket Breeding Ratio (Gross)

(Second Lithium Aluminate Zone = 13 cm - Graphite Reflector = 35cm)

Case I

$N(Li^6) = 0.018873$ $[\frac{atoms}{barn \cdot cm}]$, 90% d.f. $N(Be^9)=0.111200$ 90% d.f. (350 histories) escape prob=0.030029

$N(Li^7) = 0.002097$ $[\frac{atoms}{barn \cdot cm}]$, 90% d.f. $N(Be^9)=0.074130$ 60% d.f. (2000 ") escape prob=0.039686

$N(Be^9)=0.037067$ 30% d.f. (250 ") escape prob=0.083572

Contribution by \ Zone		First Lithium Aluminate Zone	Beryllium Zone	Second Lithium Aluminate Zone	Total Contribution
Li^6	d.f.(Be^9)=30%	0.401665 ± 0.023188	---	0.521084 ± 0.027868	0.922739 ± 0.036253
	d.f.(Be^9)=60%	0.569021 ± 0.011602	---	0.481243 ± 0.009836	1.050264 ± 0.015120
	d.f.(Be^9)=90%	0.734009 ± 0.013733	---	0.394144 ± 0.012337	1.128153 ± 0.018460
Li^7	d.f.(Be^9)=30%	0.003128 ± 0.000365	---	0.000582 ± 0.000159	0.003710 ± 0.000398
	d.f.(Be^9)=60%	0.003244 ± 0.000085	---	0.000840 ± 0.000073	0.004084 ± 0.000112
	d.f.(Be^9)=90%	0.003650 ± 0.000309	---	0.000596 ± 0.000149	0.004246 ± 0.000343
Be^9	d.f.(Be^9)=30%	---	0.003227 ± 0.000356	---	0.003227 ± 0.000356
	d.f.(Be^9)=60%	---	0.005592 ± 0.000236	---	0.005592 ± 0.000236
	d.f.(Be^9)=90%	---	0.007468 ± 0.000725	---	0.007468 ± 0.000725
Total Contribution	d.f.(Be^9)=30%	0.404793 ± 0.023190	0.003227 ± 0.000356	0.521666 ± 0.027868	0.929676 ± 0.036257
	d.f.(Be^9)=60%	0.572265 ± 0.011602	0.005592 ± 0.000236	0.482083 ± 0.009836	1.059940 ± 0.015212
	d.f.(Be^9)=90%	0.737659 ± 0.013736	0.007468 ± 0.000725	0.394740 ± 0.012337	1.139867 ± 0.018478

TABLE VII

Effect of changing the amount of Beryllium on blanket breeding ratio (gross)

(Second Lithium Aluminate zone = $\frac{\text{Case II}}{10\text{ cm}}$ Graphite Reflector zone = 38 cm)

$N(Li^6) = 0.018873 \left[\frac{\text{atoms}}{\text{barn. cm}}\right]$, 90% d.f. $N(Be^9) = 0.111200$ 90% d.f.(1200 histories), escape prob. = 0.027120

$N(Li^7) = 0.002097 \left[\frac{\text{atoms}}{\text{barn. cm}}\right]$, 90% d.f. $N(Be^9) = 0.074130$ 60% d.f.(1000 histories), escape prob. = 0.028396

$N(Be^9) = 0.037067$ 30% d.f. (350 histories), escape prob. = 0.051034

Contribution by \ Zone		First Lithium Aluminate Zone	Beryllium Zone	Second Lithium Aluminate Zone	Total Contribution
Li^6	d.f.(Be^9) = 30%	0.453065 ± 0.033712	---	0.473127 ± 0.020330	0.926192 ± 0.039367
	d.f.(Be^9) = 60%	0.582119 ± 0.023308	---	0.430398 ± 0.021812	1.012517 ± 0.031922
	d.f.(Be^9) = 90%	0.687902 ± 0.018662	---	0.373893 ± 0.021109	1.061795 ± 0.028175
Li^7	d.f.(Be^9) = 30%	0.003456 ± 0.000158	---	0.001141 ± 0.000261	0.004597 ± 0.000305
	d.f.(Be^9) = 60%	0.003133 ± 0.000059	---	0.000850 ± 0.000094	0.003983 ± 0.000111
	d.f.(Be^9) = 90%	0.003167 ± 0.000151	---	0.000669 ± 0.000120	0.003836 ± 0.000192
Be^9	d.f.(Be^9) = 30%	---	0.003443 ± 0.000320	---	0.003443 ± 0.000320
	d.f.(Be^9) = 60%	---	0.005564 ± 0.000306	---	0.005564 ± 0.000306
	d.f.(Be^9) = 90%	---	0.007231 ± 0.000377	---	0.007231 ± 0.000377
Total	d.f.(Be^9) = 30%	0.456521 ± 0.033712	0.003443 ± 0.000320	0.474268 ± 0.020331	0.934232 ± 0.039369
	d.f.(Be^9) = 60%	0.585252 ± 0.023308	0.005564 ± 0.000306	0.431248 ± 0.021811	1.022064 ± 0.031923
	d.f.(Be^9) = 90%	0.691069 ± 0.018662	0.007231 ± 0.000377	0.374562 ± 0.021109	1.072862 ± 0.028178

Table VIII

Effect of Changing the Amount of Beryllium on Blanket Breeding Ratio (Gross)

Case III

(Second Lithium Aluminate Zone = 13 cm, Graphite Reflector = 35 cm

$N(Li^6) = 0.012582$ $[\frac{atoms}{b.\ cm}]$, 60% d.f., $N(Be^9) = 0.111200$ 90% d.f., (350 histories), escape prob = 0.051242

$N(Li^7) = 0.001398$ $[\frac{atoms}{c.\ cm}]$, 60% d.f., $N(Be^9) = 0.074130$ 60% d.f. (1000 histories), escape prob. = 0.045769

$N(Be^9) = 0.037067$ 30% d.f., (350 histories), escape prob. = 0.07916

Contribution by \ Zone		First Lithium Aluminate Zone	Beryllium Zone	Second Lithium Aluminate Zone	Total Contribution
Li^6	d.f.(Be^9)=30%	0.383172 ± 0.028462	---	0.524543 ± 0.008366	0.907715 ± 0.029666
	d.f.(Be^9)=60%	0.576105 ± 0.019783	---	0.481085 ± 0.017107	1.057190 ± 0.026153
	d.f.(Be^9)=90%	0.601508 ± 0.021594	---	0.420062 ± 0.016403	1.021570 ± 0.027117
Li^7	d.f.(Be^9)=30%	0.001985 ± 0.000143	---	0.001164 ± 0.000238	0.003145 ± 0.000277
	d.f.(Be^9)=60%	0.002507 ± 0.000149	---	0.000759 ± 0.000114	0.003266 ± 0.000187
	d.f.(Be^9)=90%	0.002527 ± 0.000248	---	0.000480 ± 0.000181	0.003007 ± 0.000307
Be^9	d.f.(Be^9)=30%	---	0.004010 ± 0.000373	---	0.004010 ± 0.000373
	d.f.(Be^9)=60%	---	0.007028 ± 0.000406	---	0.007028 ± 0.000406
	d.f.(Be^9)=90%	---	0.008516 ± 0.001304	---	0.008516 ± 0.001304
Total Contribution	d.f.(Be^9)=30%	0.385157 ± 0.028462	0.004010 ± 0.000373	0.525707 ± 0.008369	0.917870 ± 0.029669
	d.f.(Be^9)=60%	0.578612 ± 0.019783	0.007028 ± 0.000406	0.481844 ± 0.017107	1.067484 ± 0.026157
	d.f.(Be^9)=90%	0.604035 ± 0.021595	0.008516 ± 0.001304	0.420542 ± 0.016403	1.093093 ± 0.027120

TABLE IX

Scalar neutron flux in unit cell, and region compositions:

Designs A and B

Region	Composition	Density Factor	Volume	Scalar Neutron Flux per source neutron $n/(cm^2$ sec. source)
V	S.S. 316	0.68	188.181	0.168503 ± 0.003065* 0.190587 ± 0.005460†
VI	S.S. 316	0.50	225.000	0.024422 ± 0.002157 0.033900 ± 0.002697
VII	S.S. 316	0.18	33.750	0.026970 ± 0.001845 0.030882 ± 0.004199
VIII	$LiAlO_2$(I)	0.90* 0.60†	123.515	0.184739 ± 0.003865 0.227907 ± 0.007504
IX	Be (I)	0.60	108.931	0.188082 ± 0.005409 0.213694 ± 0.007229
X	Be (I)	0.60	423.1234	0.137390 ± 0.003619 0.155713 ± 0.004173
XI	$LiAlO_2$(II)	0.90* 0.60†	345.670	0.040779 ± 0.001715 0.051858 ± 0.002467
XII	Graphite	0.90	1062.552	0.019336 ± 0.001385 0.028367 ± 0.002630
XIII	S.S. 316	0.95	129.937	0.004588 ± 0.000895 0.005750 ± 0.001158
XIV	S.S. 316	0.95	11.908	0.195810 ± 0.005626 0.232944 ± 0.011936
XV	S.S. 316	0.95	9.786	0.194349 ± 0.007181 0.234324 ± 0.012006
XVI	S.S. 316	0.95	40.281	0.138271 ± 0.003142 0.151719 ± 0.007139
XVII	S.S. 316	0.95	31.065	0.044182 ± 0.002649 0.054437 ± 0.004899
XVIII	S.S. 316	0.95	103.140	0.021404 ± 0.001818 0.031528 ± 0.002798

† Design A
* Design B

Figures 12 to 24 display the results of the parametric studies.

The blanket breeding ratio (gross) or equivalently, the tritium atoms production per (D-T) reaction is shown in Figures 14 to 21 for different Be density factors and for three cases:

	Second $LiAlO_2$ Zone	Graphite Reflector	$LiAlO_2$ d.f.
Case I	13 cm	35 cm	90%
Case II	10 cm	38 cm	90%
Case III	13 cm	35 cm	60%

($LiAlO_2$ and graphite zones add up to 48 cm)

Figures 20 and 21 compares the different cases. It is interesting to notice the following: (1) Tritium production in the second breeding zone falls off with the addition of Be. This is due to the reflection action of Be, since neutrons are reflected to the first breeding zone where the tritium production increases with Be addition.

(2) For the second breeding zone, tritium production increases with increased $LiAlO_2$ in it, and decreases with addition of Be (Be reflection action).

(3) Tritium production increases in the first breeding zone with Be addition, but with different slopes depending on the thickness of the second $LiAlO_2$ zone and the graphite reflector thickness. This might suggest that the second breeding zone reflects a part of the slow neutrons reaching it. Since that effect depends on the capture in the structure and does not contribute much to the blanket breeding ratio, this point was not investigated further.

(4) Tritium production increases with $LiAlO_2$ addition to the second breeding zone (Figures 12 and 20). However, as shown in Table V and Figures 21 and 13, about the same amount of breeding is obtained in designs A and B; the former with about 30% less $LiAlO_2$. This can be attributed to the larger neutron multiplication in Be offsetting the smaller optical thickness of the first $LiAlO_2$ zone. (See Table VIII).

Tritium Procution for Different Blanket Parameters: Li^7 and Be^9 Contributions, Case II

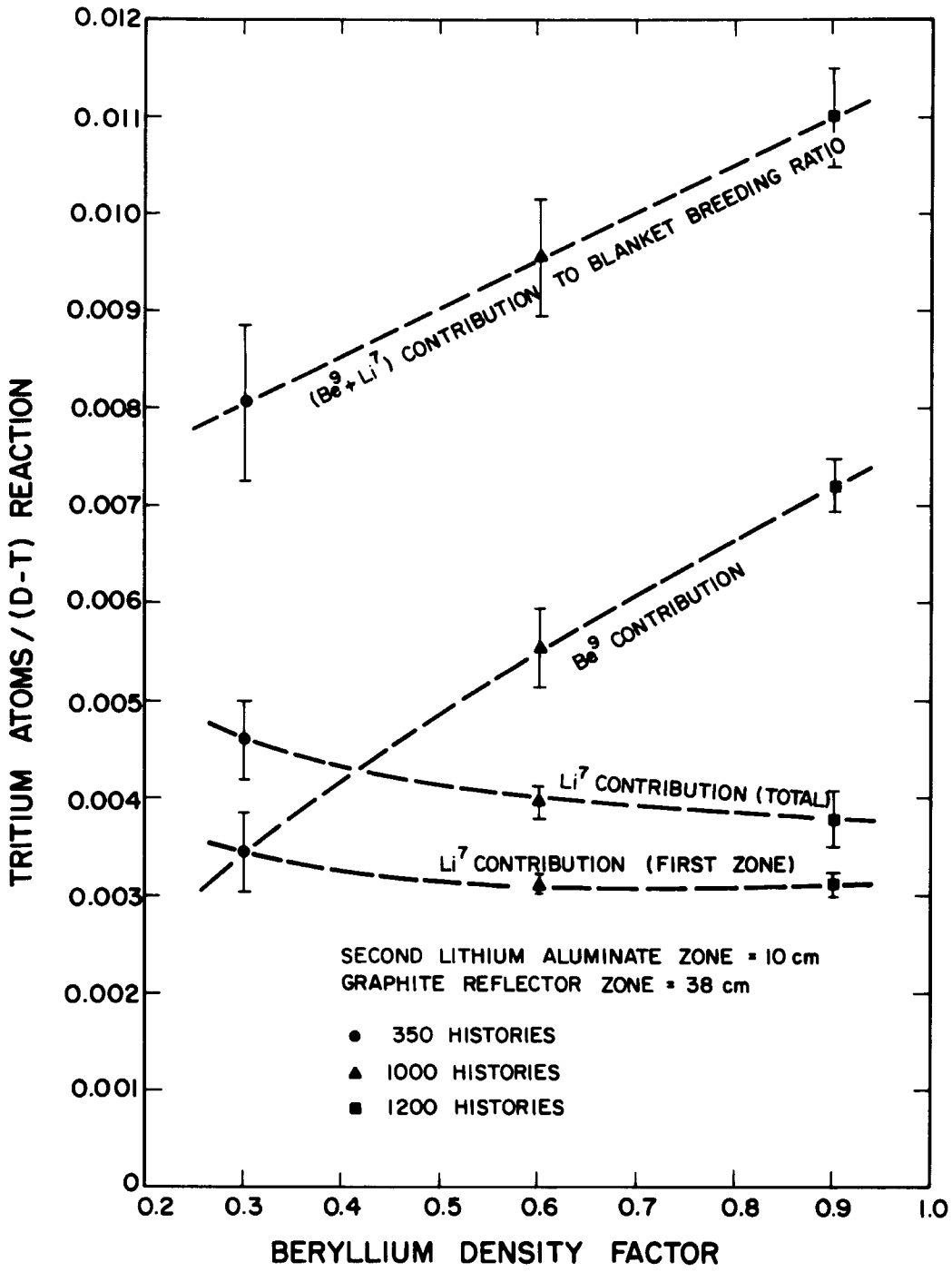

Figure 15

Tritium Production for Different Blanket Parameters: Li^7 and Be^9 contributions, Case I

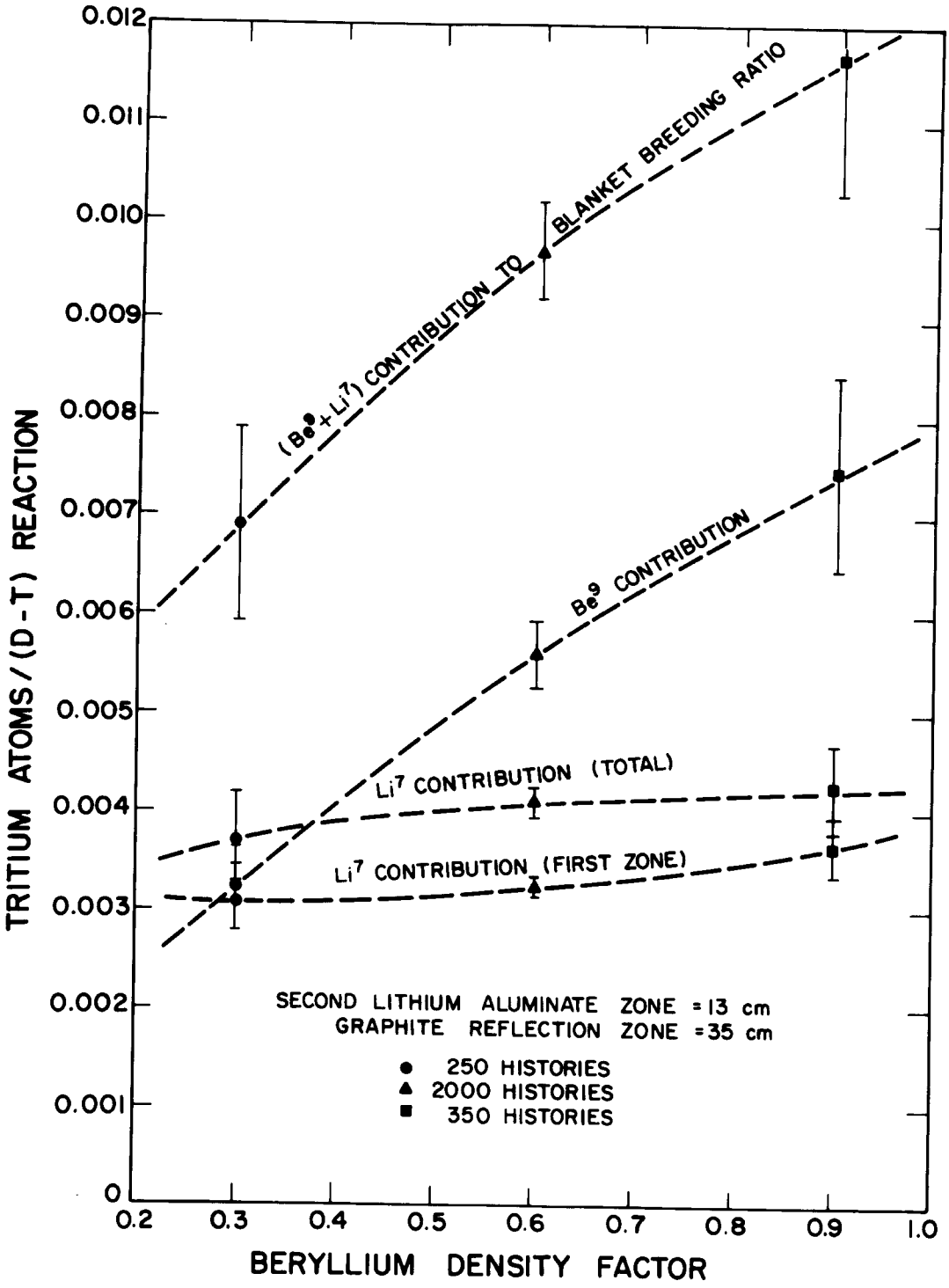

Figure 14

Tritium Production for Different Blanket Parameters: Li^7 and Be^9 Contributions, Case III

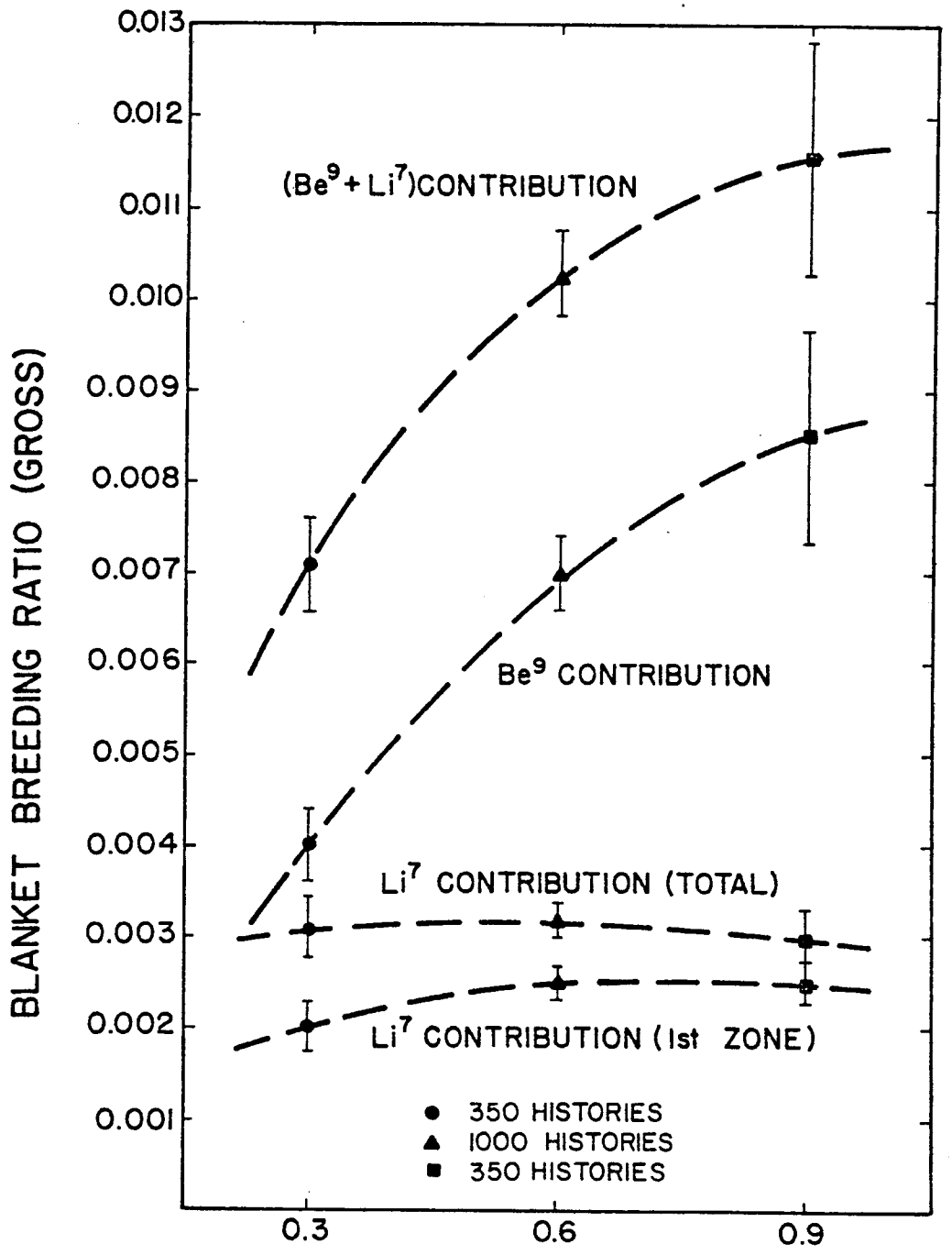

Figure 16

Tritium Production for Different Blanket Parameters: Li^6 and Total Contributions, Case I

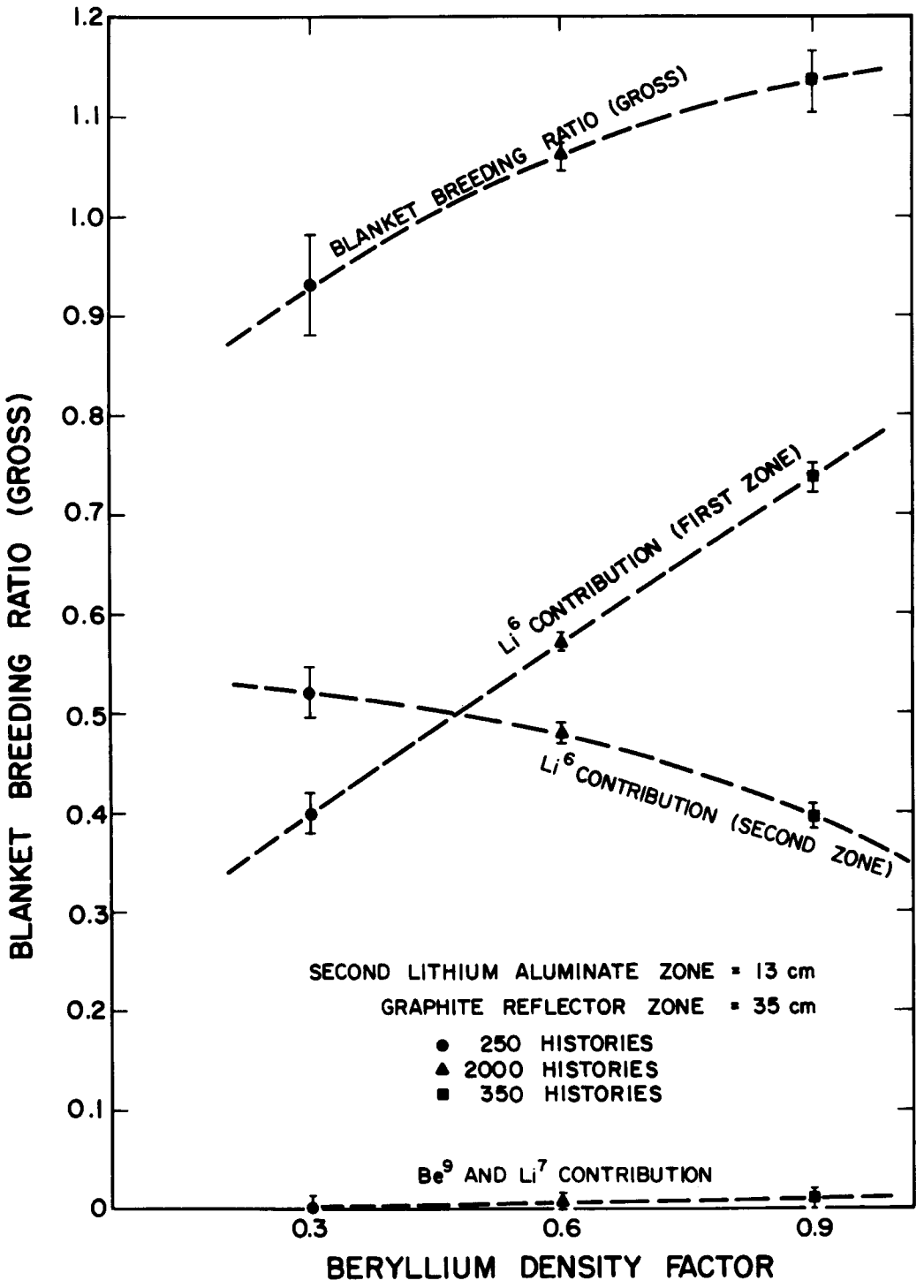

Figure 17

Tritium Production for Different Blanket Parameters: Li^6 and Total Contributions, Case II

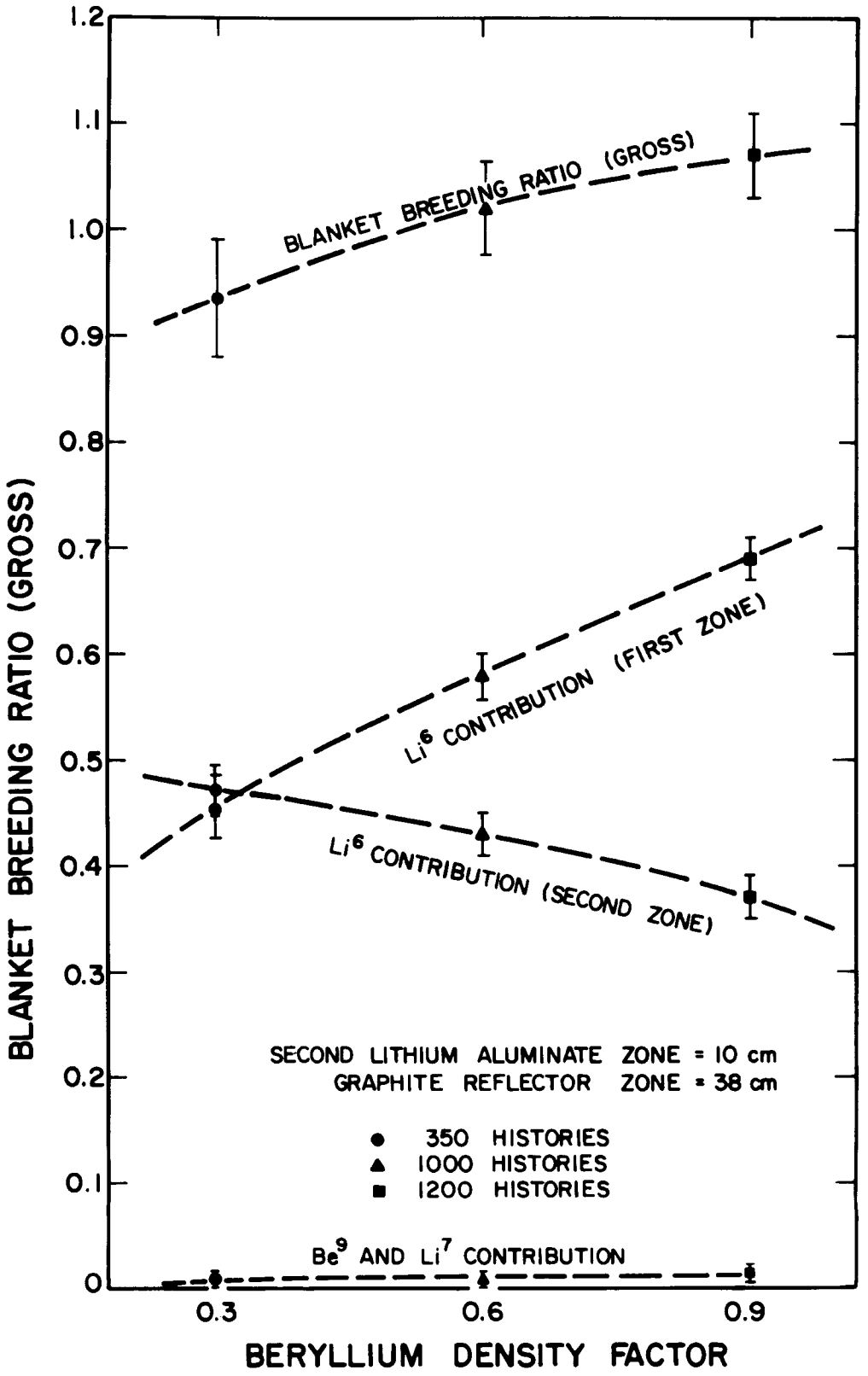

Figure 18

Tritium Production for Different Blanket Parameters Li^6 and Total Contribution, Case III

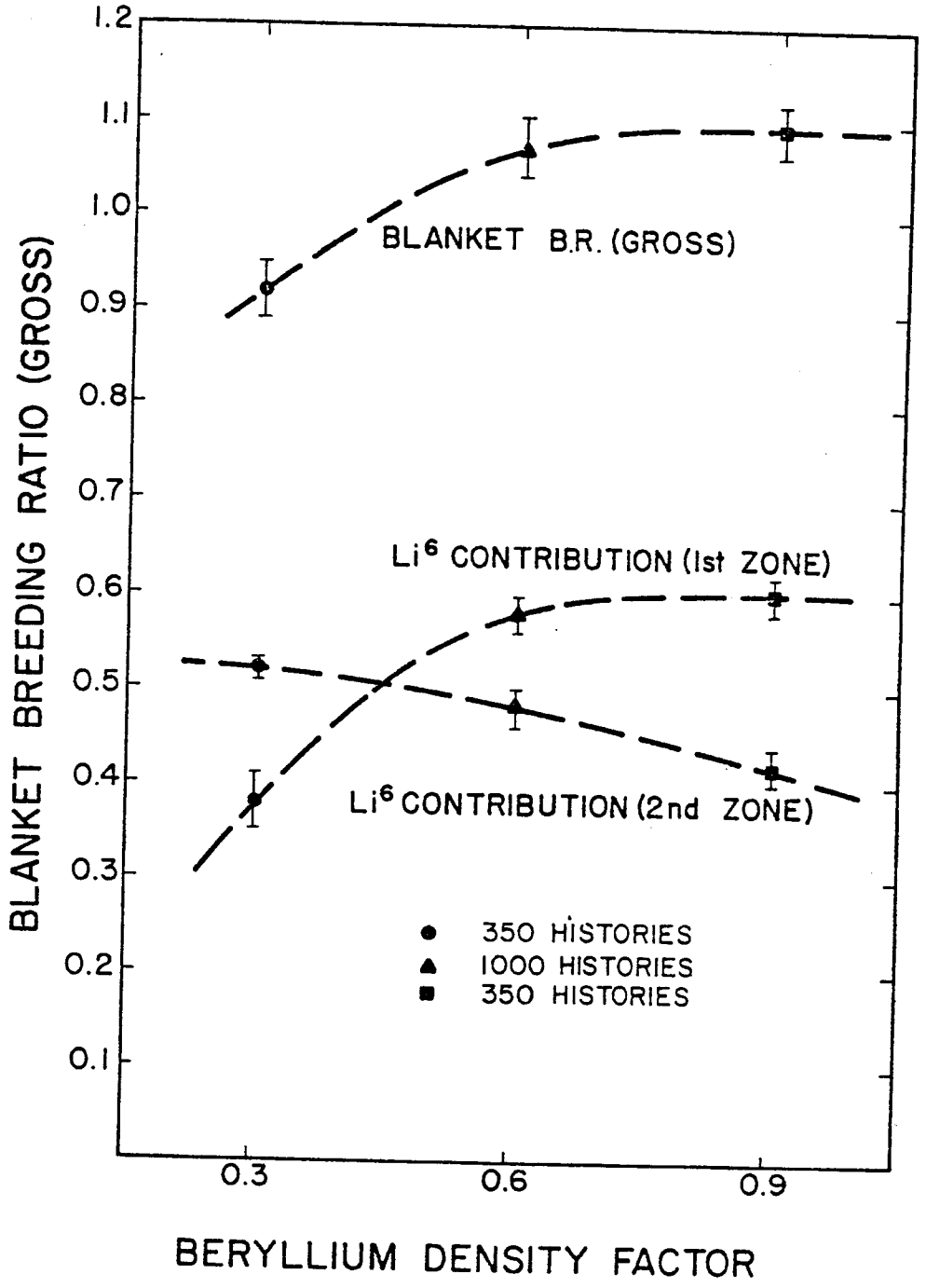

Figure 19

Comparison of Tritium Production for Parametric Study Cases

$LiAlO_2$ d.f. = 90%

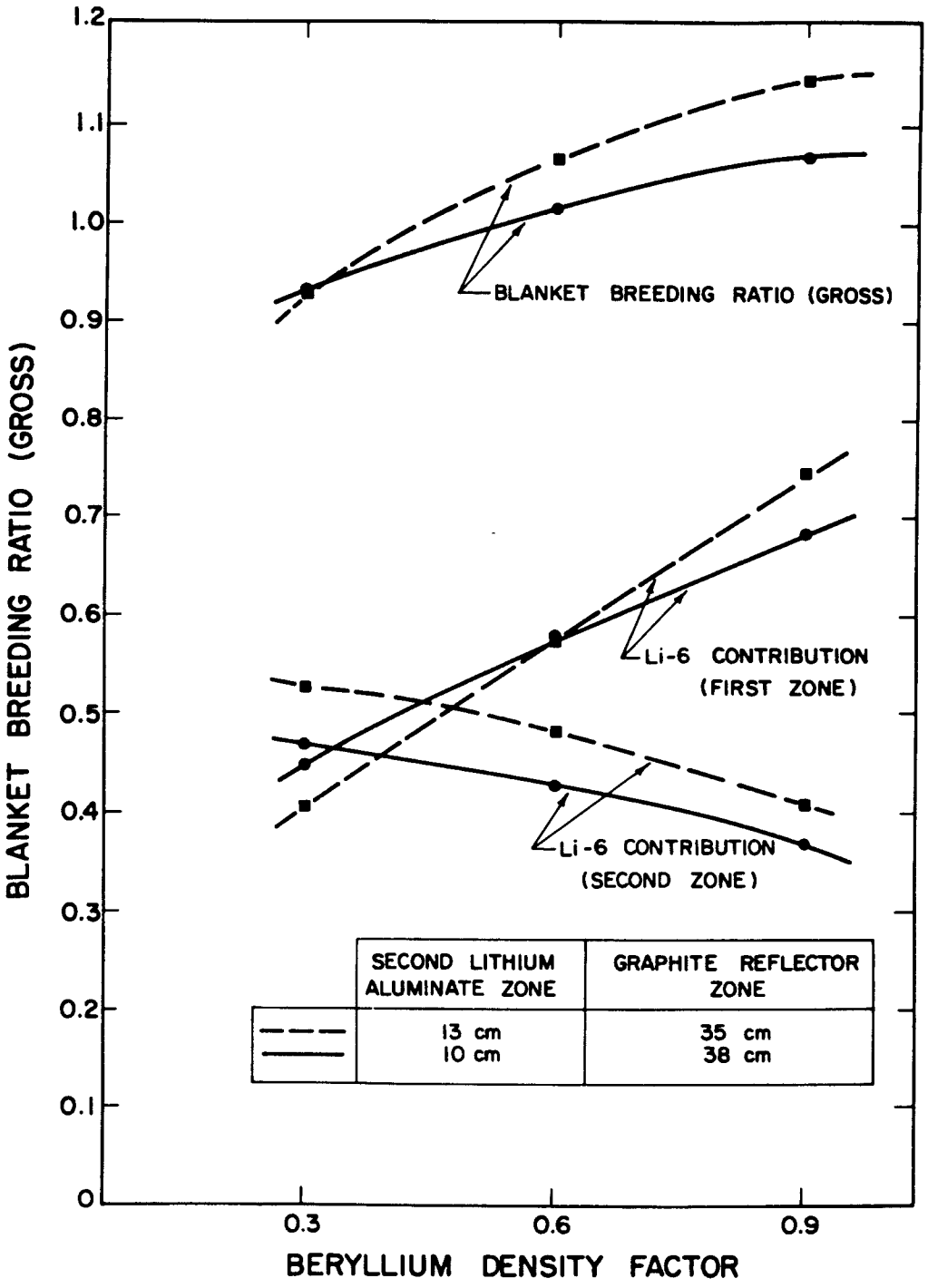

Figure 20

Comparison of Tritium Production for Parametric Study Cases

Second breeding zone = 13 cm

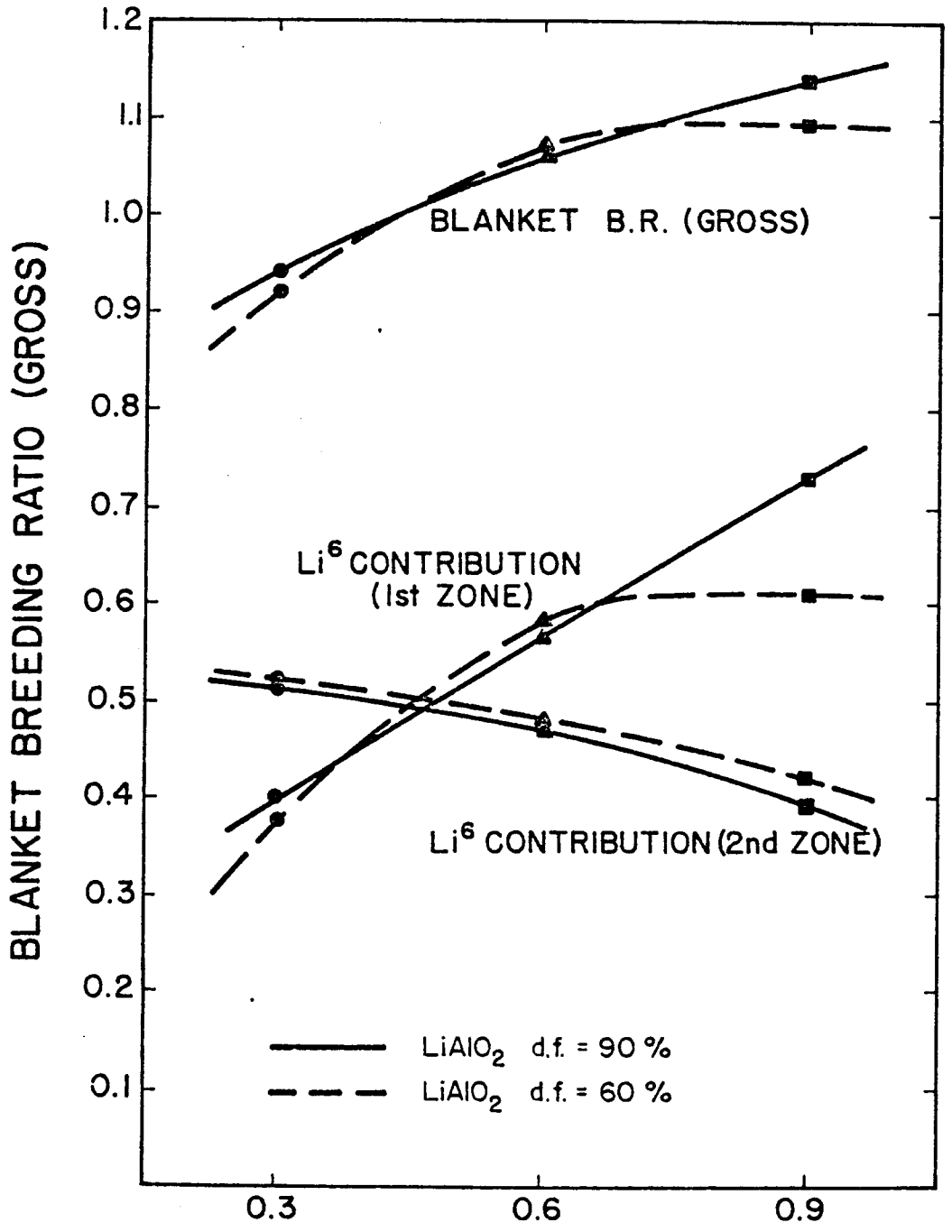

Figure 21

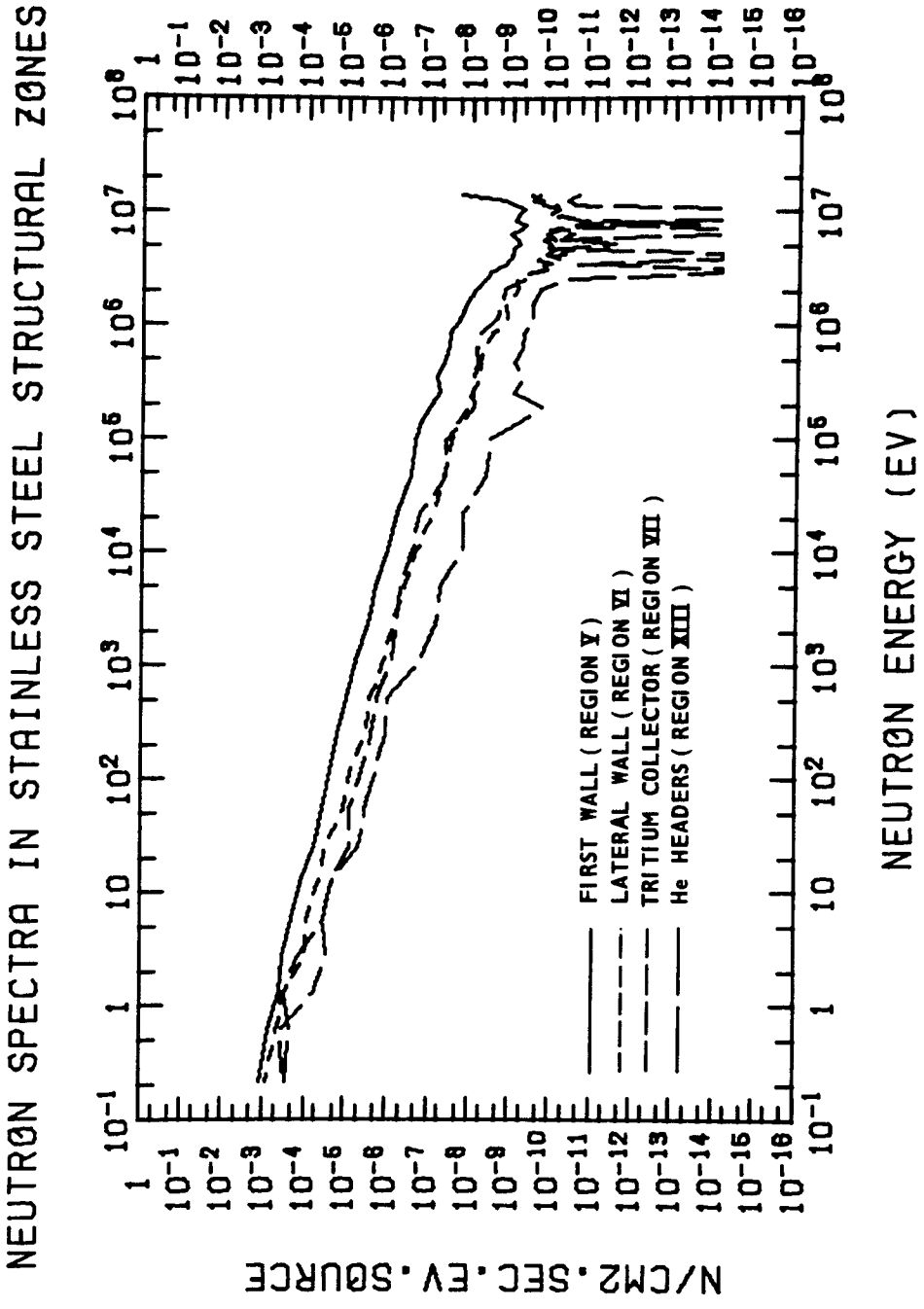
NEUTRØN SPECTRA IN STAINLESS STEEL STRUCTURAL ZØNES
N/CM2.SEC.EV.SOURCE
NEUTRØN ENERGY (EV)
FIRST WALL (REGION V)
LATERAL WALL (REGION VI)
TRITIUM COLLECTOR (REGION VII)
He HEADERS (REGION XIII)

Figure 22

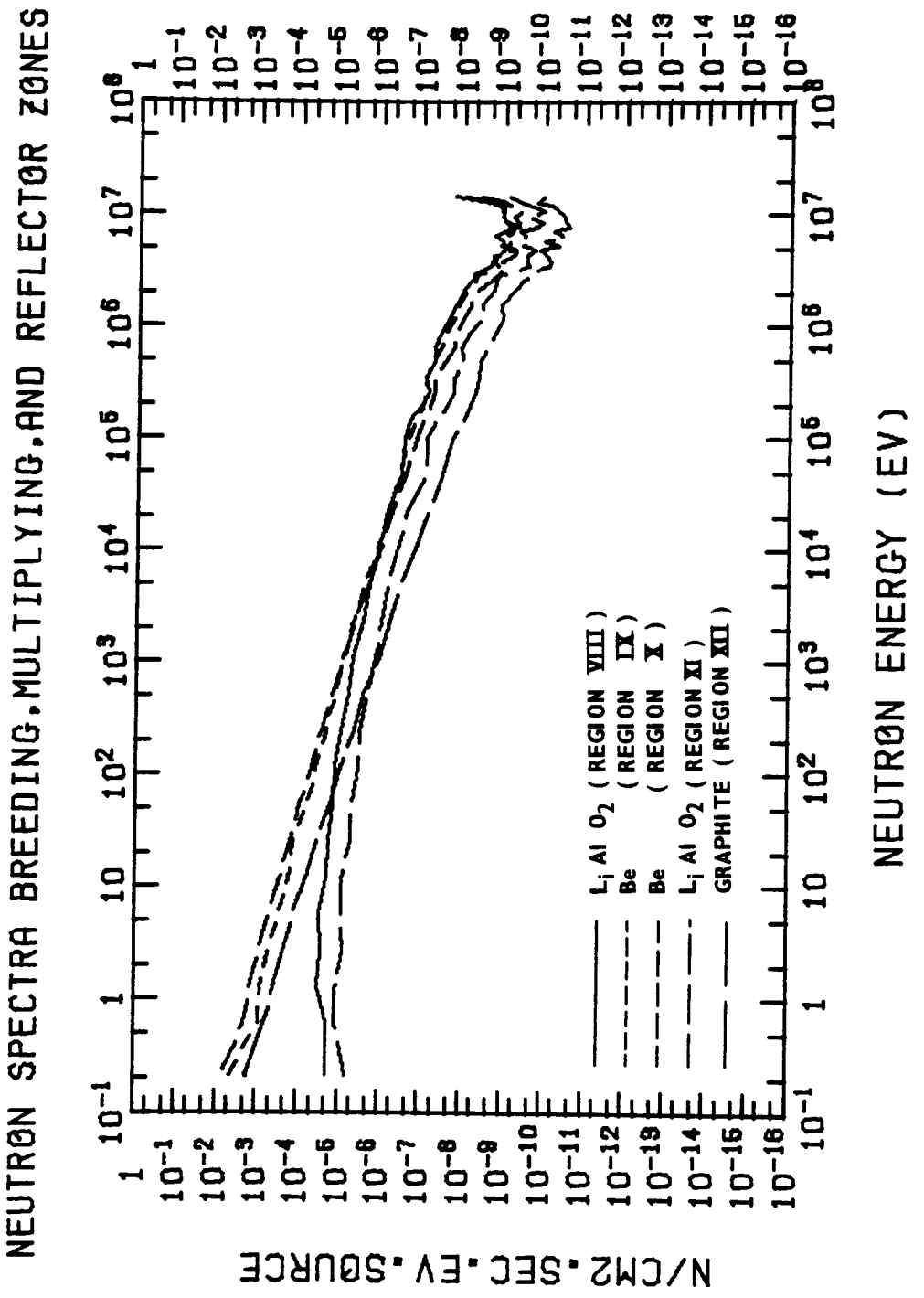
NEUTRØN SPECTRA BREEDING,MULTIPLYING,AND REFLECTØR ZØNES
N/CM2·SEC·EV·SØURCE
NEUTRØN ENERGY (EV)
Li Al O2 (REGION VIII)
Be (REGION IX)
Be (REGION X)
Li Al O2 (REGION XI)
GRAPHITE (REGION XII)

Figure 23

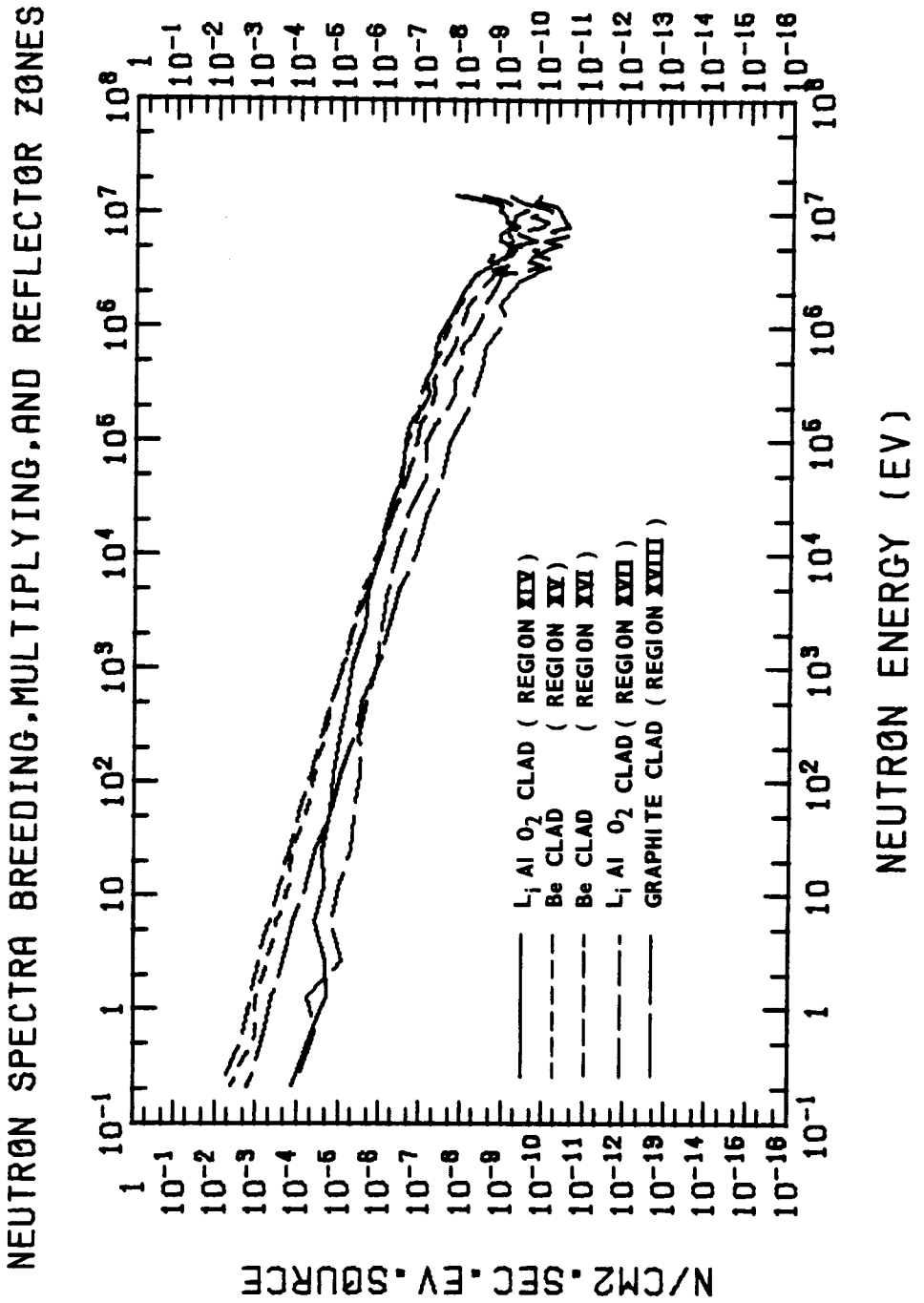
NEUTRØN SPECTRA BREEDING, MULTIPLYING, AND REFLECTØR ZØNES
N/CM2 . SEC . EV . SØURCE
NEUTRØN ENERGY (EV)
L_i Al O_2 CLAD (REGION XIV)
Be CLAD (REGION XV)
Be CLAD (REGION XVI)
L_i Al O_2 CLAD (REGION XVII)
GRAPHITE CLAD (REGION XVIII)

Figure 24

(5) In the cases treated, the blanket breeding ratio (gross) increases with Be addition. However, the slope of the tritium production from the first zone may be such that the total blanket breeding ratio may reach a maximum for a given thickness of the first breeding zone, then fall with further Be addition.

For the chosen reference design A, a blanket breeding ratio of 1.067 ± 0.026 was estimated corresponding to a neutron escape probability of 4.58%.

With a 30% increase in Be, a value of $1.140 \pm .018$ with a neutron escape probability of 3.0%, and another of 1.060 ± 0.015 with an escape probability of 3.96%, can be attained, with a 30% increase in $LiAlO_2$.

The escaping neutrons must be accounted for in the magnet shield design, or an extra breeding zone can be added to make use of them if necessary.

Neutron spectra in different regions (drawn to the same scale) are displayed in Figures 22 to 24, for the design case B.

4. COMPARISON WITH PREVIOUS CALCULATIONS

Table X shows a comparison with blanket calculations from previous studies. Particularly, the one-dimensional computation (ANISN-discrete ordinates) yields a tritium production/(D+T) reaction of 1.1835. Our iterated blanket design yields a value of 1.067 ± 0.026. It should be emphasized that the materials compositions are basically different in the one-dimensional and the three-dimensional cases: adopting exactly the materials compositions used in the one-dimensional computation could yield a tritium production per (D-T) reaction of less than one.

Specifically, if we consider a microcell, (excluding the lateral structure for 3-D calculations), the volume fractions for the 1-D and 3-D

calculations compare as follows:

		S.S.	Graphite, Be, or $LiAlO_2$	Void
Cases I and II	3-D	0.0765	0.7402	0.1833
Case III	3-D	0.0765	0.4935	0.4300
	1-D	0.05	0.45	0.5

It is apparent that the 1-D calculation underestimates the actual amount of structure present. Moreover, the lateral structure in the blanket cells was explicitly taken into account in the 3-D calculation, whilst it was placed at the back of the blanket in the 1-D calculation (zone 10 in Fig. 25) where it has almost no effect on tritium breeding. The overall effect is that it is difficult to achieve a breeding ratio larger than unity unless the ratio of structural to breeding materials is decreased. In the parametric studies, the geometry was kept constant for most of the cases, and changes in the amounts of materials were artificially accounted for by changing their number densities. The larger amount of structure present and the neutron leakage stand behind the difference between the 1-D and 3-D results, as well as heterogeneity effects.

Design A from the parametric studies is recommended as a reference design. The density factor in the $LiAlO_2$ in that design accounts for porosity and swelling requirements.

Compared to the UWMAK-I design (liquid lithium breeder-coolant), the solid gas cooled blanket shows that nearly all the contribution to breeding

TABLE X

Comparison of one-dimensional ANISN and MORSE-Monte-Carlo estimates for blanket breeding ratio (gross) for the UWMAK-I and UWMAK-II conceptual designs

UWMAK-I : Liquid lithium (natural) breeding and coolant material, (also acting as moderator).

UWMAK-II: Solid $LiAlO_2$ (90% enriched in Li^6) breeder, He coolant, S.S. 316 structure, graphite reflector, with metallic Beryllium as neutron multiplier.

Case A: 1000 histories

Case B: 2000 histories

	UWMAK-I ANISN [+]	UWMAK-I, Monte-Carlo (Unit Cell)[+]	UWMAK-II ANISN [o]	UWMAK-II Morse* Microcell Model (1500 histories)	UWMAK-II Morse* Macrocell Model
$Li^6(n,\alpha)t$	0.883481	1.025940 ± 0.016100	1.1801	1.136213 ± 0.026977	1.050264 ± 0.015210(B) 1.057190 ± 0.026153(A)
$Li^7(n,n'\alpha)t$	0.603706	0.483825 ± 0.014100	0.0034	0.004234 ± 0.000133	0.004084 ± 0.000112(B) 0.003266 ± 0.000187(A)
Be(n,t)	---	---	---	0.007645 ± 0.000355	0.005592 ± 0.000334(B) 0.007028 ± 0.000236(A)
Total Tritium production per source neutron	1.487187	1.509765 ± 0.021335	1.1835	1.148092 ± 0.026980	1.059940 ± 0.015212(B) 1.067484 ± 0.026157(A)

[+] From Reference 2 (Table V-B-10), (ENDF-III data were used for ANISN results, while ENDF-II data were used for MORSE results)

[o] From Reference 5

* This work

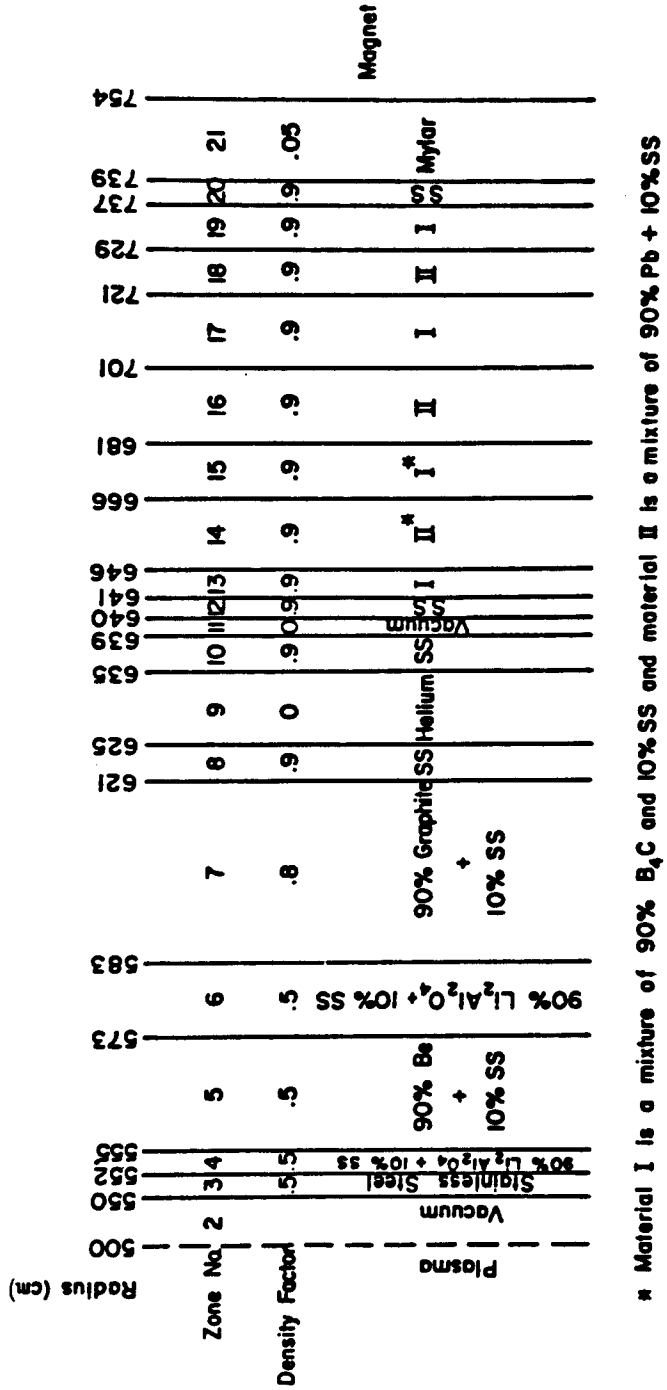

Figure25 A Schematic of UWMAK-II Blanket and Shield (One-dimensional model)

is from Li^6 in the slow neutron energy range, whereas in liquid breeder-coolant blankets, a large contribution from Li^7 and fast neutrons is present.

5. CONCLUSIONS AND RECOMMENDATIONS

Gas cooled blankets behave basically as a heterogeneous system. A blanket breeding ratio (gross) greater than one is possible by adequate optimally chosen designs. Three-dimensional calculations seem to be a necessity for such optimizations after preliminary one-dimensional studies.

A substantial escape of neutrons is noticed at the back of the blanket and must be accounted for in the shield design. In the present configuration, if the structural walls were preceded by a layer of breeding material to intercept neutrons scattered fron the Be and reflector zones, a better neutron economy with a larger breeding artio may be achieved, with a minimal size for the blanket.

An important factor not yet considered in detail is the uneven burnup of different breeding and neutron multiplication materials in different zones. The equivalent of "flux flattening" in fission reactors should be investigated since this will strongly affect tritium breeding, and may limit the blanket lifetime together with radiation damage considerations. A blanket with a "breeder and multiplication materials" management program needs to be investigated. The use of alternative structural materials that can improve the neutron economy such as Zircalloy or SAP needs further investigation.

Optimization by three-dimensional methods is necessary for solid blankets. Higher breeding ratio values should be attained to accomodate for uncertainties is cross-section data and for plant reprocessing losses.

References

1. R. W. Conn et al., "Major Design Features of the Conceptual D-T Tokamak Power Reactor, UWMAK-II", IAEA-CN-33/G1-2, Proceedings of the Fifth IAEA Conference on Plasma Physics and Controlled Nuclear Fusion Research, Tokyo, Japan, Nov. 11-15, 1974.

2. B. Badger et al., "UWMAK-I, A Wisconsin Toroidal Fusion Reactor Design," UWFDM-68, Nucl. Eng. Dept. Univ. of Wis., Nov. 1973.

3. M. A. Abdou, L. J. Wittenberg, C. W. Maynard, "A Fusion Design Study of Non-mobile Blankets with Low Lithium and Tritium Inventories," UWFDM-120, Nucl. Eng. Dept., The Univ. of Wis., Nov. 1974.

4. J. Powell, F. T. Miles, A. Aronson and W. F. Winsche, BNL-18236, Brookhaven National Laboratory, June 1973.

5. B. Badger et al., "UWMAK-II, A Helium Cooled, Stainless Steel Conceptual Tokamak Power Reactor Design," UWFDM-112, Nucl. Eng. Dept., Univ. of Wisconsin (to be published).

6. E. A. Straker, et al., "The MORSE Code with Combinatorial Geometry," SAI-72-511-LJ, (1972).

7. E. A. Straker et al., "The MORSE Code - A Multigroup Neutron and Gamma Ray Monte Carlo Transport Code," ORNL-4585, Oak Ridge National Laboratory (1970).

8. W. Engle, "A User's Manual for ANISN, A One-Dimensional Discrete Ordinates Transport Code with Anisotorpic Scattering," Report 1693, Oak Ridge, Tenn. (1967).

9. L. A. El-Guebaly and C. W. Maynard, "Monte Carlo Calculations for a Fusion Reactor Blanket and Shield," UWFDM-79, Jan. 1974.

10. R. Q. Wright and R. W. Roussin, "DLC 2/100 G Neutron Transport Code Cross Section Data generated by SUPERTOG from ENDF/B-III," July 1972 (Radiation Shielding Information Center (RSIC) at Oak Ridge National Laboratory).

11. R. Q. Wright, N. M. Greene, J. L. Lucius and C. W. Craven, Jr., "SUPERTOG: A Program to Generate Five Group Constants and P_n Scattering Matrices from ENDF/B," ORNL-TM-2679-1969.

12. M. A. Abdou, R. W. Roussin, MACKLIB, 100 Group Neutron Fluence-to-Kerma Factors and REactions Cross Sections Generated by the MACK Computer Program from DATA in ENDF Format" ORNL-TM-3995, 1974.

13. M. K. Drake, "Data Formats and Procedures for the ENDF Neutron Cross Section Library," National Neutron Cross Section Center, BNL 50274 (T-601), October 1970.

14. E. A. Straker, W. H. Scott, Jr., N. R. Byrn, "The Morse Code with Combinatorial Geometry," DNA 2860T, SAI-72-511-LJ, May 1972.

15. D. Steiner, "Analysis of a bench-mark calculation of tritium breeding in a fusion reactor blanket: the United States contribution," ORNL-TM-4177, April 1973.

16. M. B. Emmett, "The MØRSE Monte Carlo radiation transport code system," ORNL-4972, UC-32 Mathematics and Computers, February 1975.

Appendix A

Comparative Benchmark Calculation

The neutronics and photonics of conceptual fusion reactor blanket models have been treated by a number of investigators by one and two-dimensional models. Realistic designs incorporating penetrations through the blanket and shield (beam and pellet injection ports, divertor slots, etc.), leading to radiation streaming and leakage, and accounting for the heterogeneity in materials (solid blankets) necessitate the use of Monte Carlo for treating the problem in a three-dimensional way. Discrepancies were noticed between the results of three-dimensional and one-dimensional cell models for calculation (the present work). These were attributed to heterogeneity and radiation streaming and leakage effects; but it was also suggested that the discrepancies might be related to errors in the modified versions of the Monte Carlo codes used. To answer the later uncertainty, a bench-mark calculation has been carried out to compare the results obtained by the modified version of the MORSE multigroup Monte Carlo code used and those obtained by the ANISN discrete-ordinates code. Results assure the validity of the Monte Carlo calculations and strengthen faith in the results of other 3-D computations. Results of calculations are compared for tritium breeding and scalar fluxes in the different zones of the standard blanket model[15].

It was considered adequate to estimate the tritium breeding from the top six groups in the group structure used. A more thorough comparison using a 25-21 coupled neutron-gamma set is contemplated for a different design.

ENDF/B-4 data were used as shown in Table A-1. The group structure is that of table A-2. The nuclides number densities are shown in table A-3.

The response functions considered are shown in Table A-4; these include in addition to the Li^7 and Li^6 tritium producing reaction, the Niobium (n,2n) reaction.

The blanket model is shown in Fig A-1.

Table A-5 shows the case statistics for three cases solved by Monte Carlo for different numbers of histories and batch sizes.

Table A-6 compares the tritium production for the considered three Monte Carlo cases to those obtained by discrete ordinates. Even with a small number of histories for Monte Carlo, results compare favourably. It is interesting to note that the cost of Monte Carlo is not excessive, unless we use a very large number of histories.

Detail of tritium breeding per source neutron in different breeding zones is also compared in Table A-7, and that for the Nb (n,2n) reaction is also compared in Table A-8.

Table A-9 further compares the scalar fluxes per source neutron in the different blanket zones for the different study cases.

The agreement between the discrete ordinates (P_3-S_4) and Monte Carlo (P_3) results for the standard blanket model establishes the reliability of the used version of the Monte Carlo code, and the validity of our results for the three dimensional calculations. The discrepancy between the 1-D and 3-D results can be safely attributed to heterogeneity and radiation leakage effects as analyzed in our work.

Table A-1 The ENDF/B-4 Material Identification Numbers for the Nuclides Used in Computations

Nuclide	Identification Number
L_i^6	1115
L_i^7	1116
$^{93}N_b$	1164
^{12}C	1165

Table A-2 Group-Structure for the Bench-Mark Calculation*

Group	Upper Edge (ev)	Lower Edge (ev)
1	1.4920 + 07	1.3500 + 07
2	1.3500 + 07	1.2210 + 07
3	1.2210 + 07	1.1050 + 07
4	1.1050 + 07	1.0000 + 07
5	1.0000 + 07	9.0480 + 06
6	9.0480 + 06	8.1872 + 06

*These are the top six groups of the GAM-II group structure.

Table A-3 Nuclides Number Densities for the Material Mixtures of the Bench-Mark Blanket Model

Medium	Region	Constituents	Number Density
1000	1	Isotropic neutron source	---
1000	2	Inner Vacuum	---
1	3, 5	Niobium	0.055560 atoms/b. cm
2	4,6,7,8,10	Niobium	0.003334 atoms/b. cm
		Lithium-6	0.003234 atoms/b. cm
		Lithium-7	0.040380 atoms/b. cm
3	9	Carbon	0.080040 atoms/b. cm
0	11	Outer Vacuum	---

Table A-4 Response Functions Considered in Bench-Mark Problem

(Group Microscopic Cross Sections In Barns)

Group	$n(L_i^7)T$	$n(L_i^6)T$	Nb(n, 2n)
1	3.3178-01	2.5777-02	1.2178+00
2	3.4827-01	2.7325-02	1.1884+00
3	3.8789-01	3.2328-02	9.0197-01
4	4.0818-01	3.5934-02	4.9486-01
5	4.1662-01	4.0364-02	1.3498-01
6	4.2104-01	4.5534-02	1.8002-03

Figure A-1. Cylindrical Bench-Mark Blanket Model

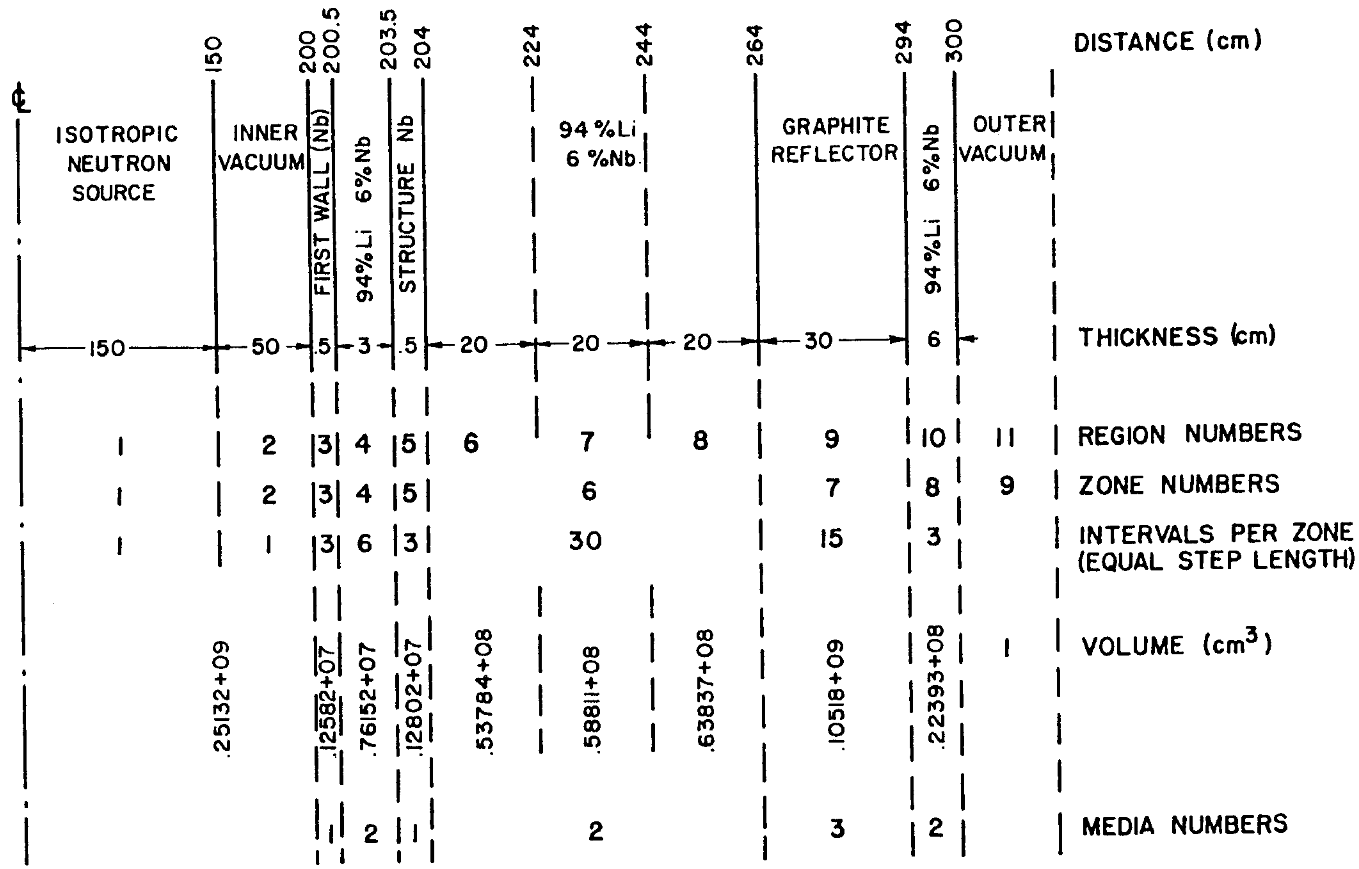

Table A-5 Case Statistics for the Monte Carlo Calculations

	Case I	Case II	Case III
Total Tritium Breeding	0.466086 ± 0.016199	0.475234 ± 0.007770	0.471649 ± 0.002770
Number of batches	4	20	100
Number of particles per batch	50	50	100
Total number of processed particles	200	1000	10000
Number of Scatterings			
Medium 1 (Nb)	137 (7.4255%)	657 (7.0028%)	6945 (7.4164%)
Medium 2 (N_b+L_i^6+L_i^7)	1547 (83.8482%)	7819 (83.3404%)	77976 (83.2685%)
Medium 3 (C)	161 (8.7263%)	906 (9.6568%)	8723 (9.3151%)
Total	1845	9382	93644
Number killed by Russian roulette	191	926	9404
Total weight	1.1276 (0.5638%)	5.7506 (0.57506%)	59.2730 (0.59273%)
Number escaped	9	74	596
Total weight	0.95797	4.8928	51.139
Leakage	0.4790%	0.4833%	0.5114%
CPU Time	14.5 sec	55.11 sec	8 min. 33.135 sec
CPU Cost	$0.38	$1.45	$13.47
Memory Usage	$0.14	$0.42	$3.70
Cost (overnight runs)	$0.82	$2.17	$17.48

Table A-6 Tritium Breeding Per Source Nuetron In Bench Mark Calculation

Top Six Groups Analysis

Method of Calculation	Cost*	Breeding in L_i^6	Breeding in L_i^7	Nb(n,2n)	Top Six Groups Total Breeding
Discrete Ordinates (ANISN) S_4,P_3	$4.34	0.003089	0.467597	0.220201	0.470686
Monte Carlo, P_3 (MORSE) 200 histories 4 batches	$0.82	0.003074 ± 0.000099	0.463012 ± 0.016199	0.209581 ± 0.011615	0.466086 ± 0.016199
Monte Carlo, P_3 (MØRSE) 1000 histories 20 batches	$2.17	0.003120 ± 0.000051	0.472114 ± 0.007770	0.210164 ± 0.005086	0.475234 ± 0.007770
Monte Carlo, P_3 (MØRSE) 10000 histories 100 batches	$17.48	0.003096 ± 0.000018	0.468553 ± 0.002770	0.215509 ± 0.001879	0.471649 ± 0.002770

*Computations carried out at the UW-UNIVAC-1110. Cost excludes charges for printed output and tape mounting. Rates are for overnight runs.

Table A-7 Comparison of Tritium Breeding per Source Neutron in Different Regions Six Group Model

Region	ANISN	MORSE (200 histories)	MORSE (1000 histories)	MORSE (10,000 histories)
		From Lithium-7		
4	0.074754	0.076577±0.003173	0.068933±0.002980	0.070808±0.001203
6	0.257909	0.258683±0.012789	0.267109±0.005510	0.255078±0.001752
7	0.096050	0.092135±0.005205	0.096917±0.003751	0.100938±0.001369
8	0.038264	0.035552±0.007830	0.038040±0.002649	0.040991±0.001131
10	0.000618	0.001097±0.000612	0.001115±0.000205	0.000738±0.000060
Total	0.467597	0.463012±0.016199	0.472114±0.007770	0.468553±0.002770
		From Lithium-6		
4	0.000482	0.000499±0.000016	0.000449±0.000020	0.000458±0.000008
6	0.001698	0.001717±0.000080	0.001760±0.000036	0.001680±0.000012
7	0.000644	0.000617±0.000027	0.000646±0.000024	0.000675±0.000009
8	0.000259	0.000233±0.000048	0.000257±0.000018	0.000278±0.000006
10	0.000004	0.000008±0.000004	0.000008±0.000001	0.000005±0.000001
Total	0.003089	0.003074±0.000099	0.003120±0.000051	0.003096±0.000018
Total Bulk	0.470686	0.466086±0.016199	0.475234±0.007770	0.471649±0.002770

Table A-8 Comparison of Nb(n,2n) Reaction per Source Neutron in Different Regions

Region	ANISN	MORSE (200 histories)	MORSE (1000 histories)	MORSE (10,000 histories)
3	0.063504	0.053162±0.007503	0.059917±0.003365	0.060889±0.001247
4	0.019615	0.019682±0.001638	0.017419±0.000768	0.018406±0.000316
5	0.046744	0.048114±0.007128	0.039595±0.003217	0.044618±0.001231
6	0.061671	0.060329±0.003739	0.063648±0.001396	0.060969±0.000455
7	0.020758	0.020035±0.002307	0.021492±0.001103	0.022147±0.000337
8	0.007800	0.008044±0.002409	0.007885±0.000662	0.008352±0.000196
10	0.000106	0.000215±0.000135	0.000208±0.000054	0.000128±0.000015
Total	0.220201	0.209581±0.011615	0.210164±0.005086	0.215509±0.001879

Table A-9 Comparison of Scaler Fluxes per Source Neutron for Different Calculations in Different Regions n/(cm^2. sec. source neutron)

Region	ANISN	MORSE (200 histories)	FSD*	MORSE (1000 histories)	FSD	MORSE (10,000 histories)	FSD
3	8.1769194-07	7.416-07+		7.470-07		7.998-07	
		6.967-07·	0.08792	7.679-07	0.04950	7.847-07	0.01943
4	7.0655137-07	7.428-07		6.883-07		6.749-07	
		7.231-07	0.04973	6.466-07	0.04309	6.678-07	0.01693
5	6.1012107-07	5.975-07		5.768-07		5.811-07	
		6.178-07	0.15214	5.240-07	0.07952	5.871-07	0.02582
6	3.3675814-07	3.290-07		3.322-07		3.336-07	
		3.366-07	0.05006	3.485-07	0.02057	3.331-07	0.00686
7	1.1189811-07	1.034-07		1.136-07		1.176-07	
		1.073-07	0.06463	1.134-07	0.04052	1.179-07	0.04374
8	4.0534499-08	4.105-08		4.125-08		4.373-08	
		3.835-08	0.23477	4.045-08	0.07174	4.342-08	0.02110
9	8.9216866-09	9.727-09		1.031-08		9.857-09	
		1.031-08	0.30092	1.036-08	0.09324	9.742-09	0.02962
10	1.8242799-09	1.977-09		2.136-09		2.225-09	
		3.307-09	0.55732	3.351-09	0.19388	2.178-09	0.08477

+ Track length estimator

· Collision Estimator

* FSD = Fractional Standard Deviation

Appendix B

The Morse Code with Combinatorial Geometry[14]

The Morse code (Multigroup Oak Ridge Stochastic Experiment) determines the distribution of particles or photons whose transport is described by the linear Boltzmann equation:

$$X(\underline{P}) = S(\underline{P}) + \int X(\underline{P}')\ K(\underline{P}' \rightarrow \underline{P})dP' \qquad (1)$$

where the components of $\underline{P}$ are the coordinates of phase space,

$S(\underline{P})$ is the source

$X(\underline{P})$ is the density of particles leaving a collision at $\underline{P}$.

The interaction processes are described by multigroup cross sections.

Monte Carlo solution of the integral equation (1) is found by estimating the terms $X_n(\underline{P})$ in the series representation where $X_o(\underline{P})$ is the source term $S(\underline{P})$ and each subsequent term is found from the previous one by sampling from the kernel $K(\underline{P}' \rightarrow \underline{P})$:

$$X(\underline{P}) = \sum_{n=0}^{\infty} X_n(\underline{P}) \qquad (2)$$

where

$$X_n(\underline{P}) = \int X_{n-1}(\underline{P}')K(\underline{P}' \rightarrow \underline{P})dP'$$

This represents transport of particles from collision to collision until the particle escapes, undergoes an absorption reaction, or is killed.

A quantity of interest λ (e.g. reaction rate) is found by integrating the product of a response function $f(\underline{P})$ and the collision density over phase space:

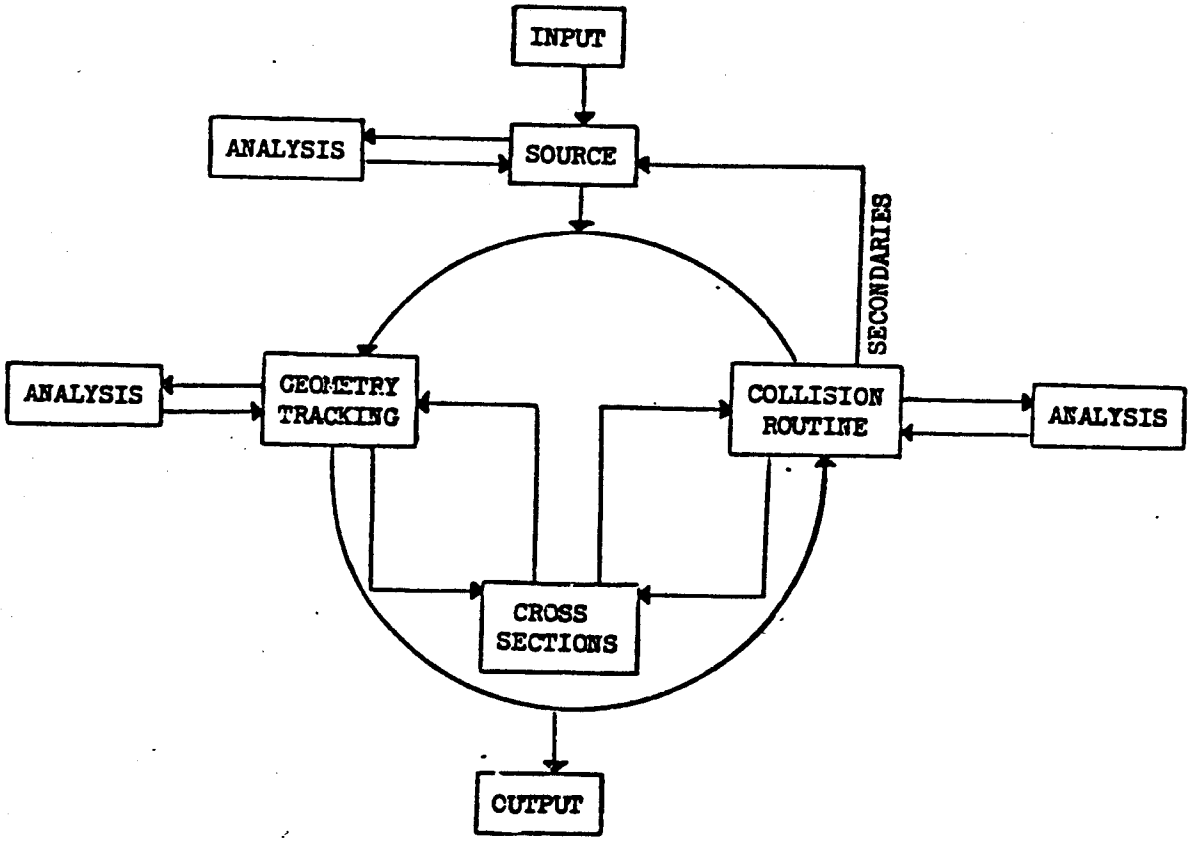

Figure B-1 Flow Diagram for the MORSE Monte-Carlo Code

$$\lambda = \sum_{n=0}^{\infty} \lambda_n \tag{3}$$

where

$$\lambda_n = \int f(\underline{P})\, X_n(\underline{P}) \cdot d\underline{P}$$

Figure A-1 shows the code modules, The "source" module is required to generate a sample of $\underline{P}$ from $S(\underline{P})$ and the "analysis" module is needed to estimate the contribution λ_n to λ. After a particle is generated, "random walk" routines generate the histories and do the major bookkeeping. The "combinatorial geometry" routine is required for tracking from collision to collision. The geometry is described as unions and intersections (OR and AND Boolean algebra operations) of primary geometrical bodies (e.g. spheres, cubes) to compose complicated geometries. The "collision" module determines energy loss, change of direction and secondary generation at a collision. The "cross section" module is needed to provide information both in the collision and tracking processes. "Analysis" of events may be required during the tracking process (track length/unit volume or boundary crossing estimators) and at the collision sites (collision density or next event estimators). The "analysis" may also make use of the "cross section" module.